Revista Ciência Agronômica, v. 51, Special Agriculture 4.0, e20207700, 2020
Centro de Ciências Agrárias - Universidade Federal do Ceará, Fortaleza, CE
www.ccarevista.ufc.br

Artigo Científico
ISSN 1806-6690

Applications of computational fluid dynamics in irrigation engineering

Aplicações de fluido-dinâmica computacional em engenharia de irrigação

Antonio Pires de Camargo[1]*, Gustavo Lopes Muniz[2], Nicolas Duarte Cano[2], Nassim Ait-Mouheb[3], Séverine Tomas[3], Diego José de Sousa Pereira[4], Rogério Lavanholi[4], José Antônio Frizzone[4] and Bruno Molle[3]

ABSTRACT - Computational fluid dynamics (CFD) techniques have become an important tool for investigating and predicting flow behavior in many industrial and engineering processes. In the last two decades, CFD has been used for the study, design, and improvement of irrigation equipment. Numerical simulations can be used to predict fluid flow, heat transfer, and chemical reactions within complex systems. The objective of this review is to provide an overview of the uses of CFD in irrigation engineering applications. The paper is organized into two main sections: fundamentals of CFD and irrigation engineering applications. The first section presents the main methods used in numerical simulations, basic equations to predict fluid flow parameters, meshing concerns, and convergence criteria. In the second section, we present applications related to friction and local head losses in pipes, liquid and solid-liquid flow simulation in drippers, chemical scaling, filters, sprinklers, direct-acting pressure-regulating valves, and Venturi injectors. The briefly described applications indicated that CFD modeling can be an accurate, quick, and feasible method for the investigation of flow parameters in irrigation pipes, fittings, emitters, and accessories. The CFD simulations can be useful for designing new products as well as for improving and optimizing existing products. Computational fluid dynamics uses in irrigation engineering must be encouraged, particularly for innovation purposes resulting from the cooperation between academia and irrigation companies.

Key words: CFD. Microirrigation. Filtration. Sprinkler. Clogging. Agriculture engineering.

RESUMO - Técnicas de fluido dinâmica computacional (CFD) se tornaram uma importante ferramenta para estudos e estimativas relacionadas ao escoamento de fluidos em diversos processos industriais e de engenharia. Nas últimas duas décadas, CFD tem sido utilizado para o estudo, projeto e aprimoramento de equipamentos de irrigação. Simulações numéricas podem ser utilizadas para estimativas de escoamento de fluidos, transferência de calor e reações químicas em sistemas complexos. O objetivo desta revisão é fornecer uma visão geral sobre uso de CFD em aplicações de engenharia de irrigação. O artigo está organizado em duas seções principais: fundamentos sobre CFD e aplicações em engenharia de irrigação. A primeira seção apresenta os principais métodos utilizados para simulação numérica, equações básicas para estimativa de parâmetros de escoamento, recomendações relacionadas a malha utilizada nas simulações, e critérios de convergência de resultados. Na segunda seção, são apresentadas aplicações relacionadas a perda distribuída e localizada de carga em tubulações, simulações de escoamento em labirinto de gotejadores com líquidos e sólidos-líquidos, precipitação de químicos, filtros, aspersores, válvulas reguladoras de pressão e injetores Venturi. As aplicações, embora descritas de modo breve, evidenciam que a modelagem utilizando CFD caracteriza um método que pode ser exato, rápido e viável para o estudo de parâmetros de escoamento em tubulações, conexões, emissores e acessórios de irrigação. As simulações empregando CFD podem ser úteis para o projeto de novos produtos, assim como para o aprimoramento e otimização de produtos existentes. Usos de CFD em engenharia de irrigação devem ser estimulados, especialmente com o propósito de inovação envolvendo parcerias entre a universidade e empresas de irrigação.

Palavras-chave: CFD. Microirrigação. Filtragem. Aspersor. Obstrução. Engenharia agrícola.

DOI: 10.5935/1806-6690.20200097
Editores do artigo: Professor Daniel Albiero - daniel.albiero@gmail.com e Professor Alek Sandro Dutra - alekdutra@ufc.br
*Author for correspondence
[1]Faculdade de Engenharia Agrícola, Universidade Estadual de Campinas/UNICAMP, Campinas-SP, Brasil, apcpires@unicamp.br (ORCID ID 0000-0001-5164-2634)
[2]Faculdade de Engenharia Agrícola, Universidade Estadual de Campinas/UNICAMP, Campinas-SP, Brasil, gustavolopesmuniz@yahoo.com.br (ORCID ID 0000-0002-6045-611X), nicduarte_91@hotmail.com (ORCID ID 0000-0002-1649-3060)
[3]French National Institute for Agriculture, Food, and Environment, Joint Research Unit "Water Management, Actors, Territories," Department of Waters, University of Montpellier, Montpellier 34196, France, nassim.ait-mouheb@inrae.fr (ORCID 0000-0003-0099-0983), severine.tomas@inrae.fr (ORCID ID 0000-0002-8139-1810), bruno.molle@inrae.fr (ORCID ID 0000-0003-0268-6117)
[4]Escola Superior de Agricultura Luiz de Queiroz/ESALQ, Universidade de São Paulo/USP, Piracicaba-SP, Brasil, diego_sousa1502@hotmail.com (ORCID 0000-0002-0160-0249), rogeriolavanholi@hotmail.com (ORCID ID 0000-0002-9142-4380), frizzone@usp.br (ORCID ID 0000-0002-4251-1496)

INTRODUCTION

Irrigated agriculture accounts for approximately 20% of the total agricultural land and contributes to 40% of the global food supply. On a global scale, irrigation uses represent about 70% of the total water withdrawn. Competition for access to water resources among multiple water users is expected to intensify owing to the 60% increase in food production required by the predicted global population of nine billion people by 2050 (KURIAN; REZA, 2015). The demand for freshwater, energy, and food will increase significantly over the next decades. The combination of modern irrigated agriculture with other techniques are key elements for food security, economic development, and sustainable management of natural resources.

Irrigation engineering is the analysis and design of systems that optimally supply the right amount of water to the soil at the right time to meet the needs of the plant system (WALLER; YITAYEW, 2016). Efforts to modernize irrigation engineering can contribute to optimizing water productivity and resource efficiencies (e.g., water, energy, labor, costs, and other resources for agriculture). Achievements may be achieved through improvements and innovation in irrigation system equipment, design, operation, and management.

Computational fluid dynamics (CFD) can be used to predict fluid flow, heat transfer, and chemical reactions within complex systems. The dissemination of CFD tools in industry and academia, particularly in the last two decades, resulted from the rapid advances in computer hardware, developments in numerical algorithms and physical models, and development of CFD software that is more user-friendly and capable of coupling complex phenomena (NORTON, 2013). There are many CFD applications in agriculture and the food industry (BARTZANAS *et al*., 2013; LEE *et al*., 2013), and these numerical simulations provide a cost-effective way of carrying out equipment and process design and optimization (BARTZANAS *et al*., 2013).

Computational fluid dynamic techniques have become an important tool for examining and predicting flow behavior in many industrial and engineering processes (PALAU-SALVADOR *et al*., 2006). One of the first scientific references about the use of CFD techniques to examine flow behavior in irrigation equipment was presented in 2004 (PALAU SALVADOR *et al*., 2004). Since then, many investigations have used CFD to study, design, and improve irrigation equipment.

The development of irrigation equipment in a conventional approach involves the manufacturing and testing of several prototypes. Each prototype may require hydraulic calculations, a three-dimensional model, mold manufacturing, assemblage, and performance evaluation by experimental means. The traditional method is time- and labor-consuming as well as expensive. In addition, experiments in laboratory or field trials are also both time- and labor-consuming, and their results are affected by the measurement uncertainty of instruments and other uncontrolled variables. In this aspect, CFD has become part of the engineering design and analysis environment of many laboratories and companies because of its ability to predict the performance of new designs or processes prior to manufacturing or implementation (BARTZANAS *et al*., 2013). For development stages, computational simulations can be particularly useful to reduce resources that impact development costs. Nevertheless, experimental data will always be essential for the validation of numerical simulations and to confirm the performance of irrigation equipment.

The objective of this review is to provide an overview of the uses of CFD in irrigation engineering applications. The paper begins with the fundamentals of CFD, and then the applications are introduced. The first section presents the main methods used in numerical simulations, basic equations to predict fluid flow parameters, meshing concerns, and convergence criteria. In the applications, we presented friction and local head losses in pipes, liquid and solid-liquid flow simulation in drippers, chemical scaling, filters, sprinklers, direct-acting pressure-regulating valves, and Venturi injectors.

FUNDAMENTALS ABOUT COMPUTATIONAL FLUID DYNAMICS

Numerical resolution by the finite volume method

The main methods used in numerical simulation codes are finite volume, finite differences, and finite elements. The finite difference method discretizes the continuous equations at the nodes of a predefined mesh by calculating each partial derivative using a truncated Taylor series. Nonlinear equations are obtained by linking the value of the unknowns at a node to the values of these same unknowns at neighboring nodes. The finite element technique discretizes the domain using simple geometric elements (triangles, 2D rectangles and tetrahedrons, and 3D hexahedrons). This method is suitable for modeling complex geometries. The form of the equations is replaced by the weak form in which the unknowns are calculated, for example, with a linear combination of basic functions of which the support is one element.

Most commercial CFD software (e.g., ANSYS Fluent, COMSOL Multiphysics, and OpenFoam) are based on the finite volume method. This method consists of discretizing the flow domain into a multitude of control volumes (cells) and then performing balances (mass, energy, momentum, etc.) on these small volumes. For this reason, the resolution shows volume integration. The advantage of this method is that everything that comes out of a volume goes into another. In practice, each continuous equation is integrated for each control volume, and then the Green-Ostrogradsky theorem is used to transform some surface integrals into volume integrals in the case of permanent flow. The next step is to discretize the unknowns of the problem as well as the differential operators of the equations. These mathematical operations provide a discretized equation that links the variables of one cell to those of the neighboring cells. The set of these discretized equations finally forms a matrix system.

Equations and models

Several equations and models enable numerical simulation to predict fluid flow parameters. The Navier-Stokes equations concerning the fluid mechanics are solved using a finite volume method, implemented with numerical simulation codes. The integration of the discrete equations, coupled with pressure/velocity parameters, is carried out by an algorithm. The differential form of the continuity equation and Navier-Stokes momentum equations for compressible Newtonian fluid can be written as (POPE, 2000):

$$\frac{\partial \rho}{\partial t} + \frac{\partial \rho\, u_i}{\partial x_i} = 0$$

The equations for momentum:

$$\frac{\partial \rho\, u_i}{\partial t} + \frac{\partial \rho\, u_i\, u_j}{\partial x_j} = -\frac{\partial \rho}{\partial x_i} + \frac{\partial \tau_{ij}}{\partial x_i}$$

where ρ is the fluid density (kg m^{-3}).

The instantaneous velocity $u_i\ (x_j;\ t)$, where *(i = 1; 2; 3)* and the pressure $p\ (x_j;\ t)$ at any time *t* and at any point x_j *(where j = 1; 2; 3)* of the flow field are treated independently of the temperature. The viscous stress tensor, *ij*, is proportional to the symmetric part of the deformation rate tensor (Newtonian fluid) with the Stokes hypothesis, and is given by:

$$\tau_{ij} = \mu\left(\frac{\partial u_i}{\partial u_j} + \frac{\partial u_j}{\partial x_i} - \frac{2}{3}\frac{\partial u_k}{\partial x_k}\delta_{ij}\right)$$

where μ is the dynamic fluid viscosity (kg m^{-1} s^{-1}) and δ_{ij} is the Kronecker symbol.

For turbulent flow, Reynolds-averaged Navier-Stokes equations (RANS) are currently introduced. The standard k-ε model is typically used for most engineering calculations, even if it has been developed for fully turbulent flows. The RNG k-ε model generally improves the accuracy for rapidly strained and swirling flows. These features make the RNG k-ε model more accurate and reliable for a wider class of flows than the standard k-ε model. The realizable k-ε model is effectively applied in various flow simulations, including vortex steady shear flow, free flow containing jet and mixed flow, pipe flow, boundary layer flow, and segregated flow. All these models calculate the turbulent stress using the isotropic turbulent viscosity assumption.

The Reynolds stress model (RSM) considers the effects of streamline curvature, swirl, rotation, and rapid changes in strain rate in a more rigorous way. Other more complex simulations, such as large eddy simulation (LES) or direct numerical simulation (DNS) models, can be found. However, they still require substantially finer meshes than those typically used for Reynolds-averaged Navier-Stokes equations (RANS) calculations. As a result, the computational cost involved with LES or DNS is usually some orders of magnitude higher than that for steady RANS calculations in terms of memory and central processing unit (CPU) time. Therefore, high-performance computing is required for LES or DNS, particularly for industrial applications.

Another tricky problem dealing with irrigation flow modeling is the multiphase flow description for sprinkler irrigation (the water and the air must be modeled). The jet is composed of optically dense turbulent zones and zones in which the liquid is dispersed in the form of three-dimensional fragments of very varied shapes and sizes, making it very difficult to characterize them. The presence of a liquid continuum at the nozzle outlet and the large variety of scales present in the flow make it particularly difficult to model using the classical approaches reported in the literature for two-phase flow modeling. Such approaches can be divided into two categories based on (1) tracking liquid/gas interfaces, and (2) those without interface reconstruction (GOROKHOVSKI; HERRMANN, 2008). The former estimates the position of the liquid/gas interfaces at a given position and instant by the volume of fluid and level-Set-type algorithms (MÉNARD *et al.*, 2007). These methods require sufficiently fine discretization of the calculation domain to capture the liquid/gas interface positions and frequently result in long computation times. Among the methods that do not use interface reconstruction, one can distinguish Eulerian/Lagrangian and Eulerian approaches (NIJDAM *et al.*, 2006). The gas flow is described by an Eulerian approach, while the droplet

characteristics (position, velocity, and size) are resolved in the calculation domain (PATANKAR; JOSEPH, 2001). This method assumes the existence of individual dispersed droplets, which does not correspond to the situation observed experimentally for sprinkler jets at the nozzle outlet. In addition, the presence of non-spherical liquid fragments makes it difficult to apply this type of modeling. In the Eulerian approach, the two-fluid model considers the two phases as two continuous interpenetrating media. The conservation equations are solved for each phase and contain the terms of interaction between phases that are difficult to model. An alternative is to consider the conservation equations of the two-phase mixture, which is represented as a single fluid of variable density. The main asset of this approach lies in its ability to describe the flow in a continuous way, both in the liquid core at the nozzle outlet and in the dispersed part of the spray. In this formulation, the slip velocity is related to flow variables to take into account interactions between the two phases (STEVENIN *et al*., 2016).

Meshing concerns

The numerical codes can use structured, unstructured, or hybrid meshes. A structured mesh is generally composed of quadrilateral meshes in two dimensions (2D or surface mesh) and hexahedral meshes in three dimensions (3D or volume mesh), while an unstructured mesh is composed of quadrilateral or triangular meshes in 2D and hexahedral or tetrahedral meshes in 3D. In a hybrid mesh, the meshes close to the walls are quadrilaterals in 2D and hexahedrons in 3D, and the meshes in the rest of the domain are triangles in 2D and tetrahedrons in 3D. Near the wall, it is necessary to refine the mesh to model the flows in this zone where the gradients of various quantities are high. During the simulation, it is necessary to demonstrate the independence of the results with the size and geometry of the resolution meshes.

Convergence criteria

While solving fluid flow equations, the residuals are evaluated for each variable of the equations, for example, pressure or velocity. Convergence is determined from these residues. There are no absolute criteria to evaluate it, but it is recommended to examine not only the residues and their evolution, but also the values of the calculated quantities. In addition, the number of iterations depends on the total number of meshes of the geometry and the model parameters.

The validation of results with experimental data is always required.

APPLICATIONS OF COMPUTATIONAL FLUID DYNAMICS ON IRRIGATION ENGINEERING

Friction and local head losses in pipes

Irrigation systems are designed to transport water from a source through a network of pipes to irrigated crops. Flow velocities, friction losses, and minor losses are some of the flow parameters that must be accurately predicted to achieve proper operational conditions and acceptable uniformity of water application over the irrigated area. Minor losses are particularly important in the design of microirrigation subunits owing to the large number of emitters installed along the laterals (BOMBARDELLI *et al*., 2019; PROVENZANO *et al*., 2016; SOBENKO *et al*., 2020; VILAÇA *et al*., 2017).

In irrigation applications, friction losses are usually estimated by the Darcy-Weisbach equation or by empirical equations (e.g., Hazen-Williams, Flamant). Friction losses can also be determined experimentally by evaluating segments of straight pipes to obtain pairs of points that result in a curve of pressure loss as a function of flow rate values.

The presence of a singularity (e.g., emitter, fitting, accessory) in a segment of a pipe causes a local pressure loss, which is often expressed as a fraction K_L of the kinetic head. Sometimes, local head losses are also expressed in terms of the equivalent length of the pipe, and the total head loss is estimated using friction loss equations, considering the physical length of the pipe plus the sum of equivalent lengths. In addition, when a segment of a pipe has singularities, the experimental procedure first consists of determining the total head loss. Second, local head losses are obtained by the difference between the total head loss and the friction loss.

Local head losses have also been estimated using dimensional analysis approaches (BOMBARDELLI *et al*., 2019; DEMIR *et al*., 2007; PERBONI *et al*., 2015; VILAÇA *et al*., 2017; WANG *et al*., 2018; ZITTERELL *et al*., 2013) and machine learning-based algorithms (MARTÍ *et al*., 2010; SOBENKO *et al*., 2020). Sometimes, the geometrical characteristics of the devices are complex, which complicates the identification of the relevant physical information that must be part of mathematical or computational models. If an important physical quantity is not considered as an input variable, the accuracy of predictions can be impaired.

The variety of irrigation equipment used is enormous. Laboratory experiments to determine pressure losses are both time- and labor-consuming. In addition,

most empirical models reported in the literature are valid for specific conditions. Computational fluid dynamic techniques can be useful for simulating flow parameters such as friction losses and local head losses.

An experimental and numerical study on irrigation laterals was carried out by Palau-Salvador *et al*. (2006) for the prediction of local losses due to the protrusion of on-line emitters. Seven models of emitters attached to a polyethylene (PE) pipe of 13.21 mm internal diameter were evaluated within a range of Reynolds number from 2774 to 20817. The geometries were drawn using Pro-Engineer software. The three-dimensional mesh was generated using Gambit, and the simulations were run using ANSYS Fluent 6.1. For the turbulent flow conditions, the authors used the RSM. A graphical comparison between simulated and measured local losses is presented, but prediction errors are not depicted. Computational fluid dynamics revealed the flow behavior around the protrusion area and might be useful for future designs and improvements in the geometry of the emitter connection to the pipe by seeking to reduce flow disturbances and minor losses.

A few studies have been carried out on CFD simulations for the prediction of friction losses and local head losses in small-diameter PE pipes with integrated cylindrical drippers. Provenzano et al. (2007) simulated a single commercial emitting-pipe of 13.76 mm internal diameter using ANSYS Fluent 6.1. The CFD technique enabled simulation with reasonable accuracy head losses in PE pipes in the range of Reynolds numbers typical of the low-turbulence regime $(4000 < R < 20000)$. The best accuracy was obtained using the YS low-Reynolds turbulence model (YANG *et al*., 1993). The friction head loss was simulated in a segment of PE pipe without emitters, resulting in errors from experimental data up to 7.4%. The error between the simulated and measured values of the local head loss coefficient varied from 6.0% to 15.5%. The comparison between simulated and measured values indicates the possibility of estimating the friction losses in PE pipes and local losses due to the emitter connections using CFD techniques, requiring experiments only for validation purposes.

Celik *et al*. (2015) simulated a 3D model of a cylindrical dripper of 4 L h^{-1} nominal discharge, spaced at 25 cm along a pipe of 16 mm internal diameter. The solid model was generated using the SolidWorks Parametric Solid Modelling Design, and the CFD simulation was achieved using SolidWorks Flow Simulation. The values of head loss were simulated by changing the inlet pressures from 50 to 200 kPa. Validation was achieved using the empirical equations reported in previous studies. The maximum error between the simulated and reference values of head loss reached 8.8%.

Small-diameter PE pipes with integrated cylindrical drippers were also investigated using CFD and dimensional analysis approaches (WANG *et al*., 2018). The pipe internal diameter varied between 6.4–14.8 mm and the Reynolds number ranged from 3000–74000. Twelve configurations of pipe internal diameter, inside emitter diameter, and emitter length were simulated. Four models of the emitting-pipes were evaluated by experimental means for validation purposes. The geometries were generated using the Gambit software. The realizable k-ε model was used to simulate turbulent flow, and the flow near the wall of the pipe was simulated with the standard wall function. The errors between the simulated and measured values of total head loss varied within 3.4%– 2.8%. The authors also mentioned that numerical simulations accurately reflected the effect of temperature changes on local head losses, saving time and labor, and avoiding the influence of uncontrollable factors that are expected to occur while conducting laboratory experiments.

The prediction of total head loss in drip irrigation laterals with integrated cylindrical drippers was also performed by Demir et al. (2019), who compared the results obtained by using different turbulent models and wall functions. Two models of emitting-pipes of 13.6 mm internal diameter had their pressure loss curves determined in the laboratory within the range $4728 < R < 22457$. The 3D models, the mesh structures, and the numerical simulations were generated/performed using ANSYS Fluent 16.2. In the CFD analysis, the standard k-ε, RNG k-ε, realizable k-ε, RSM with linear pressure-strain turbulence models, and standard wall function, non-equilibrium wall function, and enhanced wall treatment were considered. The curves of the total head loss as a function of flow velocity were plotted for the comparison of the experimental data and simulated values. The most accurate predictions were obtained by the RSM turbulence model with LPS using the standard wall function, but all the evaluated turbulent models combined with the standard wall function or the non-equilibrium wall function presented satisfactory accuracy. However, poor predictions were obtained when combining any of the turbulent models with enhanced wall treatment.

Liquid and solid-liquid flow simulation in drippers

Drippers (or emitters) are important components of drip irrigation systems that are installed along polyethylene pipes (i.e., the laterals) and are responsible for controlling the discharge to apply water evenly on the soil. Non-pressure compensating (NPC) and pressure-compensating (PC) drippers are the main groups of commercially available drippers. Some models of PC drippers integrate additional features to provide non-

leakage control (CNL) for pulse irrigation or the anti-syphon (AS) mechanism for subsurface drip irrigation.

The use of labyrinth channels as a mechanism of energy dissipation stands out in the drippers' design. A labyrinth consists of a narrow and tortuous channel with several baffles that generate head losses and ensure discharge regulation. The cross-sectional area of labyrinth channels generally ranges from 0.5 to 2.0 mm² to achieve discharges that usually vary within 0.5–8.0 L h^{-1}. Drippers designed based on labyrinth channels are commonly used in drip irrigation systems because of their low cost, simple structure, and efficient hydraulic performance (LAVANHOLI *et al*., 2020; YU *et al*., 2019; ZHANG *et al*., 2010).

While NPC drippers have only a labyrinth channel for discharge control, the PC drippers typically consist of a labyrinth and a flexible membrane (i.e., the diaphragm) that deforms according to the pressure to control the flow resistance. Another important characteristic of PC drippers is the activation pressure, which represents the pressure at which the nominal discharge and flow-compensating mechanism begins to operate consistently (NARAIN; WINTER, 2019).

The dimensions and shape of the labyrinth channels have significant impacts on the hydraulic performance and the resistance of drippers to clogging. Relating the constructive characteristics of labyrinths to their hydraulic performance is usually a complex process in which hydraulic parameters, such as head loss and discharge, cannot be determined by means of the trivial hydraulic equations used in the study of pressurized pipes. Basically, the energy is dissipated in two forms in the labyrinth channel: one occurs in the straight sections of the channel and is related to the friction losses during fluid flow, and the other is related to minor losses resulting from sudden changes in flow direction, vortices, and singularities at the inlet and outlet sections of the labyrinth (LAVANHOLI *et al.*, 2020; SHAMSHERY *et al.*, 2017; ZHANG *et al*., 2011).

The hydraulic performance of emitters is usually related to their pressure-discharge equation (i.e. $q = k\,h^{x}$). A low value of x indicates that the emitter discharge is less sensitive to the inlet pressure and water temperature effects. The maximum length of the lateral lines in the microirrigation subunits may increase as the emitter flow exponent decreases, and it may be economically beneficial (FRIZZONE *et al*., 2012). Additionally, compact drippers (i.e., small dimensions) require less material for their production and are preferable to achieve low manufacturing costs.

The resistance of drippers to clogging (i.e., anti-clogging performance) relies on the drippers' design and water quality. The narrow flow path of the drippers can be easily clogged by particles, inorganic matter, chemical precipitation, biofilm development, and other impurities. Several current studies have been investigating and trying to improve the geometrical characteristics of the flow path to enhance the resistance of drippers to clogging.

In terms of suspended solids in irrigation water, clogging may occur when (1) suspended solid particles (isolated or aggregated) are larger than the flow path, and (2) when the flow velocity is low enough to allow particle settlement and the gradual reduction of the flow cross-sectional area (LAVANHOLI *et al*., 2018; LI *et al*., 2008). The high turbulence within the labyrinths enables the formation of vortices that are important mechanisms for energy dissipation and discharge control. There are geometric characteristics that promote the development of more-intense vortices, increase the turbulence and the head loss, decrease the exponent of flow, and finally result in better hydraulic performance and more compact emitters. The turbulent flow condition helps to dissipate energy and facilitates the transport of sediments out of the labyrinth channel, avoiding clogging (LI *et al*., 2006). Some low-speed regions associated with vortices (i.e., recirculation zones) are prone to sediment deposition and should be avoided to enhance particle transport through the emitter flow path (*FENG et al*., 2018). In addition, increasing the velocity near the wall of the flow path could act as a self-cleaning mechanism, preventing particle deposition and reducing clogging (LI *et al*., 2008).

Computational fluid dynamics has been a useful tool in the study of the flow behavior of the labyrinth channels of drippers. Although CFD is a powerful and effective tool to investigate and support the design of labyrinth channels, such numerical simulations usually demand considerable computational capacity and experimental data for validation purposes.

Computational fluid dynamics was used to estimate the pressure-discharge relation of labyrinth channels of triangular, rectangular, and trapezoidal shapes (WEI *et al*., 2006). The three designs were commercially available NPC drippers of nominal discharge ranging from 2 to 4 L h^{-1} and were evaluated under inlet pressure heads varying from 5 to 25 m. According to the authors, the transition from laminar to turbulent flow in channels with an area of approximately 1.0 mm² occurs at low Reynolds numbers (100–700). The standard k-ε model was used in the simulations, and the effects of surface roughness near the wall were neglected. The 3D tetrahedron meshes and simulations were performed using ANSYS Fluent. Relative errors from the measured discharges varied from 1.58% to 5.41%.

The range of Reynolds number values in which the flow regime changes from laminar to turbulent seems to be an issue for small labyrinth channels (LI *et al*., 2006). In pressurized pipes, the flow is laminar if $R_e \leq 2000$, turbulent if $R_e \geq 4000$, and transitional flow occurs if $2000 < R_e < 4000$. Thus, for a 2 L h^{-1} dripper squared cross-sectional area of about 1 mm^2, the average value of the Reynolds number is approximately 551 at the labyrinth; hence, the flow should be classified as laminar. However, in the literature, the flow regime is often considered to be turbulent owing to the complexity of milli-channels in a labyrinth form (NISHIMURA *et al*., 1984), which are composed of several baffles. There are not yet appropriate theories to calculate the critical Reynolds number in such geometries. Nishimura et al. (1984) studied a complex symmetrical corrugated channel or tube. They found that the transition from laminar flow to turbulent flow occurs when the Reynolds number system reaches 350. In addition, it should be noted that other authors describe the 3D flow in labyrinth micro-fluidic systems as a chaotic advection in a laminar regime. An unsteady velocity field can lead to very complicated trajectories, called chaotic trajectories. For these reasons, experimental validation is important to compare the different hypotheses or models of CFD. In order to validate the CFD hypotheses, it is important to compare them with experimental fluid mechanical methods, and only a few experimental studies have been conducted in drippers. This lack of experimental studies can be justified by the complexity of the geometry.

Prototypes of an NPC flat dripper with an arc-type labyrinth were manufactured using stereolithography (ZHANG *et al*., 2007). Like most commercially available drippers, the prototype consists of an inlet filter grid, the channel, and the outlet water groove (Figure 1). The laminar and the RSM were applied to the simulations using ANSYS Fluent 6.2. The inlet pressure varied from 40 to 160 kPa. Although the Reynolds number was less than 2000, the turbulence model provided better accuracy than the laminar model for predicting discharges as a function of inlet pressures. Relative errors from the measured discharges varied from 7.7% to 16.2% for predictions using the laminar flow model, and from 2.3% to 6.8% using the RSM.

A solid-liquid two-phase turbulent model describing the flow within drippers was studied by Qingsong *et al*. (2008). Three novel NPC drippers with nominal discharge ranging from 4.3 to 6.6 L h^{-1} were designed and evaluated in this study. ANSYS Fluent was used to solve the two-phase turbulent model. The standard k-ε model was used for the water flow simulation. The granular $CaCO_3$ material available in the software was chosen to represent the suspended solid particles in the irrigation water, but the simulations did not consider possible interactions among the suspended particles. Eight combinations of particle sizes (45–425 µm) and concentrations (250–2000 mg L^{-1}) were evaluated by numerical and experimental means at an inlet pressure head of 10 m. Simulated and experimental values of discharges under clogging risk conditions were compared. Numerical simulations showed the moving trace of suspended solids within the channels that provided some visual evidence of zones that were more prone to clogging (Figure 2).

Computation fluid dynamics was used to analyze the fluid movement in labyrinth flow paths, and a two-dimensional digital particle image velocimetry visual display system was developed to validate the numerical simulations (LI *et al*., 2008). Gambit was used for gridding, and the standard k-ε model and the standard wall function were used for the water flow simulation in ANSYS Fluent. In terms of clogging resistance, the authors recommended that the dripper design should eliminate regions of low velocity by creating smooth arc connections in these regions. They also mentioned that the optimal arc radius will vary according to the operating pressure. In addition, the turbulence intensity is referred to as an interesting flow variable that describes the energy dissipation properties of emitters and interferes with the transport capacity of sediments within the channels.

The flow characteristics of three labyrinth designs operated under micro-pressures (10–50 kPa) were evaluated by numerical simulations and experimental means (LI *et al*., 2009). The configuration and the tools for numerical simulation were similar to those of Li *et al.* (2008). The relative errors between the simulated and measured discharges were less than 10%, indicating that the CFD simulations were also feasible for operating pressures lower than the most usual values (i.e., >50 kPa).

A method based on the passage rate of particles was proposed to evaluate the clogging resistance of emitters by numerical simulation using ANSYS Fluent 6.2 (ZHANG *et al*., 2010). The passage rate of particles was defined as the ratio of the number of particles passing through the labyrinth channels to the total particle number entering the inlet of the labyrinth channels. The stochastic trajectory model based on the Lagrangian reference frame was used to track the velocity and position of each particle at each time step, and then the state of the particles after a number of time steps was predicted. Simulations assumed spherical inert particles of 100 µm diameter and 2,500 kg m^{-3} density. The RSM was adopted in the turbulent flow simulations. Sixteen designs of trapezoidal labyrinth channels were simulated and evaluated experimentally. The passage rate

Figure 1 - 3D model (A) and numerical model (B) of the emitter with an arc-type labyrinth, and the prototype integrated to the pipe (C) (ZHANG *et al*., 2007)

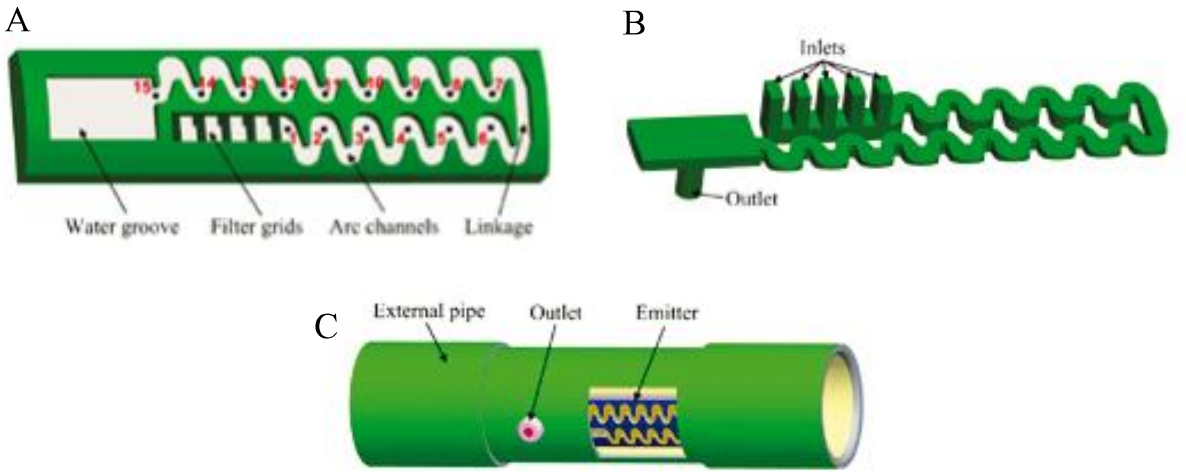

Figure 2 - Numerical models, moving trace of suspended solids, and zones of solids deposition for the three emitters: (A) eddy channel; (B) pre-depositing channel; (C) round-flow channel (QINGSONG *et al*., 2008)

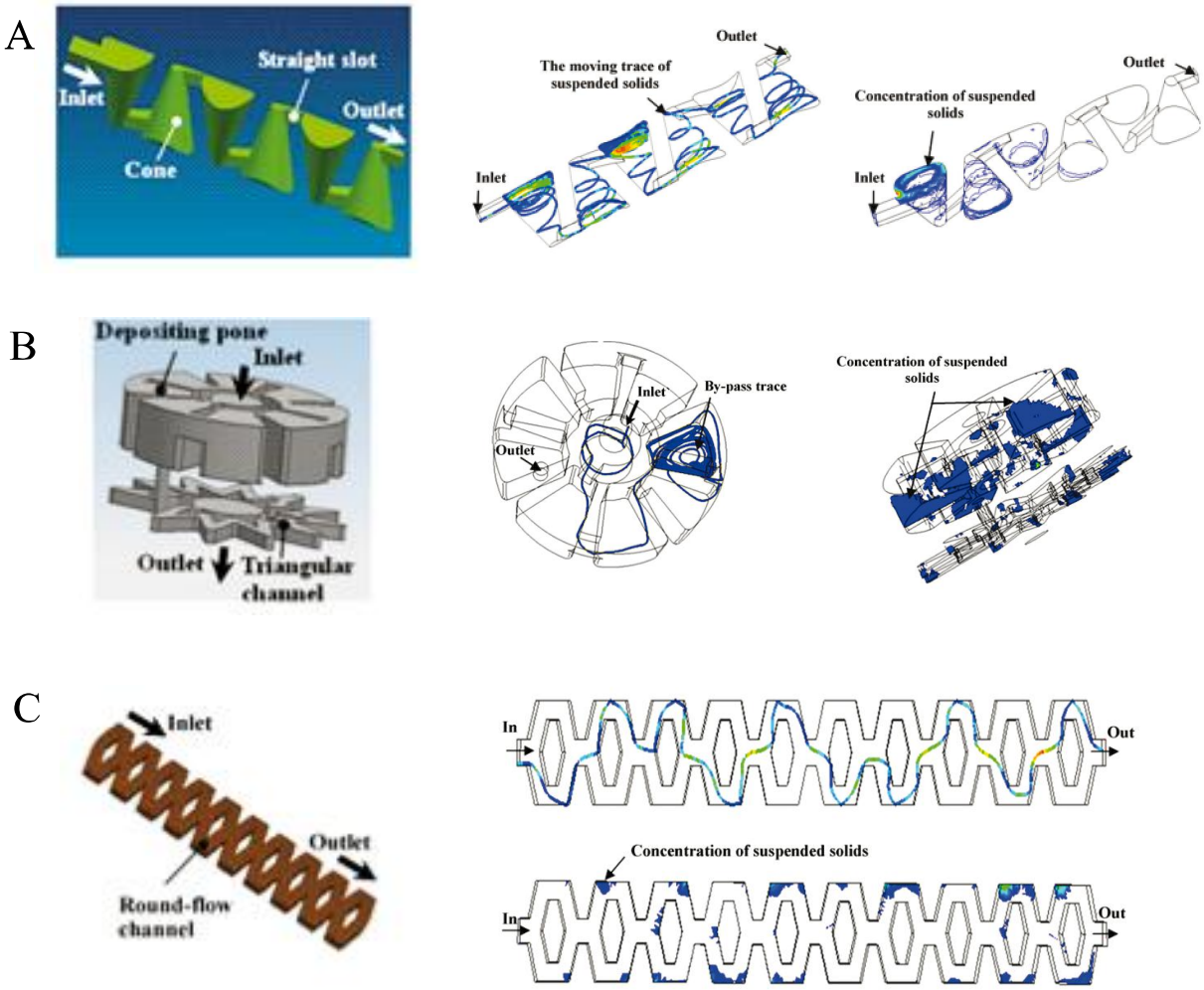

of particles was affected by several design parameters, but the labyrinth tooth angle was the most important. A regression mathematical model was fitted to predict the passage rate of particles as a function of design parameter dimensions.

The standard k-ε model and the Large Eddy Simulation method (LES) were applied to analyze the flow characteristic in a NPC cylindrical dripper (WU *et al*., 2013). The relative errors from the measured discharges were 4.7% and 10.3% for the LES and the standard k-ε model, respectively. The LES model was more effective in simulating the flow characteristics in the flow path of drip irrigation emitters, but it also presented higher computational requirements than the standard k-ε model.

The flow behavior of suspended particles with diameters of 0.01, 0.02, 0.04, 0.05, 0.06, and 0.08 mm was simulated using ANSYS Fluent Particle Tracking (LI *et al*., 2013). The LES and standard k-ε model were used to solve the two-phase flow in the labyrinth paths. The discharge errors from the measured values were 8.8% and 10.6% for the LES and the standard k-ε model, respectively. Although the accuracy obtained with the LES model was higher than the standard k-ε model, the former demanded more time to solve the numerical calculation. According to the authors, the standard k-ε model could sufficiently satisfy the accuracy requirements for calculation and analysis. The tracing ability of the particles with 0.01 mm diameter was good enough to be used for a single-phase test, but for a two-phase test, particles should be larger than 0.04 mm to achieve satisfactory accuracy.

The fluid-structure interaction (FSI) analysis using CFD was evaluated on the simulation of the pressure-discharge curves of PC drippers (WEI *et al*., 2014). In these problems, there are challenges to couple interactions between the fluid flow and elastic diaphragm, as indicated by the number 2 in Figure 3A. Simulations were run using the ADINA software. Adaptive mesh repair was adopted to refine the distorted fluid mesh. The incremental method and displacement-pressure finite element formula were used for the nonlinear analysis of the incompressible material. The shear stress transport (SST) K-ω turbulence model was used for the fluid analysis, while the contact analysis method and Neo-Hookean Mooney-Rivlin rubber material model were adopted for the structure analysis. Emitter samples were manufactured using rapid prototyping techniques and evaluated in the laboratory to experimentally obtain the pressure-discharge curve. The emitters' discharges were accurately predicted using FSI analysis (deviation from experimental values < 2.5%). The reported results are limited to testing pressures lower than 50 kPa, which usually corresponds to the minimum pressure recommended for the use of PC drippers. Although encouraging results were obtained, trials at higher pressures would be required for practical applications.

The flow characteristics of NPC drippers with exponents of flow smaller than 0.5 were investigated within pressures from 10–150 kPa to understand why these drippers present a low sensitivity of discharge to pressure variations (ZHANGZHONG *et al*., 2015). Three-dimensional models were drawn using the Pro/ Engineering software. Simulations used the standard k-ε model and the standard wall function. Digital particle image velocimetry was used to validate the flow velocity fields. The maximum relative error of the simulated from measured flow velocities was 11.9%, indicating that the standard k-ε model provided acceptable results. The study enabled the identification and explanation of a type of pressure-compensating mechanism that occurs when pressure varies and changes in the flow characteristics can be observed. When the operating pressure increases, the area of the low-speed vortex region expands incrementally, resulting in shrinkage of the width of the flow cross-section in the mainstream region, which finally inhibits the increase in the emitter discharge due to the pressure increase. Finally, the lower the flow exponent, the greater the regulation degree of the flow cross-section in these emitters and the higher the compensating effects, which consequently improves the discharge control mechanism. A similar methodology was used to evaluate the geometrical parameters of 13 models of M-type fractal flow path design (ZHANGZHONG *et al*., 2016). Flow velocities and turbulent intensity changes due to modifications in the width, length, and depth of the flow path were quantified.

A numerical technique based on the Lattice Boltzmann method (LBM) to model the flow through an NPC dripper of a rectangular flow section was proposed by Falcucci *et al*. (2017). Most CFD applications to drippers are based on turbulent models solved by the finite volume method or the finite element method. The LBM is based on the Lattice Boltzmann equation that simulates transport phenomena through the evolution of density distribution functions. It allows for the fluid flow simulation without turbulence modelling. The LBM consists of solving the macroscopic fluid dynamics through a kinetic approach, in which molecular details are neglected, except for those necessary to ensure mass, momentum, and energy conservation at the macroscopic level. According to the authors, the main advantages of LBM, with respect to conventional CFD, are its simpler dynamics and higher computational performance.

A computational fluid dynamics-discrete element method (CFD-DEM) coupling approach was employed to investigate the mechanism of emitter clogging caused by particles with sizes of 65, 100, and 150 μm (YU *et al*., 2018). The discrete element method (DEM) uses Newton's

Figure 3 - Model of the pressure-compensating dripper (A), fluid mesh (B), and sectional view of the adaptively refined mesh near the diaphragm (C) (WEI *et al*., 2014)

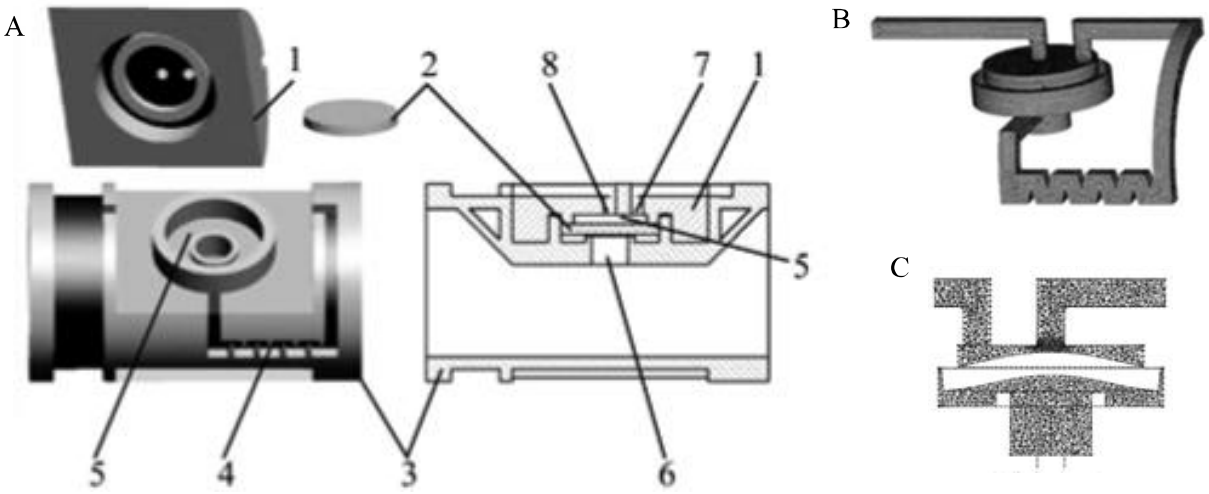

laws of motion to measure single particle motion and group distribution of the disperse phase. The CFD-DEM coupling approach was adopted to investigate the movement and distribution of sediment in the flow and the possible blocking positions caused by granules. Particle tracking velocimetry (PTV) was also utilized to follow the trajectories and velocity of a single particle. Simulations were run using ANSYS Fluent 12.0 and EDEM 2.2. Particles of 65 μm were mainly influenced by drag forces being carried in the mainstream flow, while the 150 μm particles were mainly affected by inertial forces, and hence were easily trapped in the vortex areas. For sediments of size 100 mm, the drag force was close to the inertial force, which enhanced the probability of sand entering the vortex. The CFD-DEM approach was also used to evaluate the influence of the dentation angle of the labyrinth channels on the hydraulic performance and clogging resistance of NPC drippers (YU *et al*., 2019).

A flat NPC dripper of 1.38 L h^{-1} was evaluated, and optimization attempts were proposed by Feng *et al*. (2018). The meshes were hexahedral structured meshes divided by ANSYS ICEM software. Particle motion was simulated using a standard Eulerian-Lagrangian multiphase flow model. The accuracy of the simulation with the LES model was the highest, followed by the RNG k-ε model, while it was lowest for the standard k-ε model. Although the LES model had the highest accuracy, it also had the highest computational requirements. Based on the analysis of the calculation accuracy and computational requirements, the RNG k-ε turbulence model was the most suitable model for simulating the flow field in the emitter's flow path. According to the authors, the first approach to improve clogging resistance consists of eliminating the low-speed region related to the vortices, where the sediments can easily deposit and enlarge the mainstream area to enhance the transportation capacity of particles through the flow path of the emitter. Eliminating the vortex area in the flow path could seriously decrease the hydraulic performance of the emitter (i.e., increase the flow exponent of the pressure-discharge relationship) and increase the cost of emitter manufacturing (i.e., longer paths to obtain low discharges). The second approach, which seems to be more suitable, consists of promoting fully developed vortices to improve the washing ability near the walls. Vortices are an efficient mechanism for the energy dissipation necessary to attain hydraulic performance, while the whirling motion of the vortex enhances the self-cleaning ability, improving clogging resistance.

The flow in labyrinth-channel irrigation drippers was investigated using micro-PIV methods and CFD modeling (AL-MUHAMMAD *et al*., 2019). The detection and characterization of the vortex zone in a milli-labyrinth-channel are presented and detailed in this paper. According to this study, the RSM model can be considered a reliable model for predicting and characterizing the flow in the labyrinth channel. The results obtained by the RSM model are in good agreement with the experimental results, with a difference of 5% in the mean velocity prediction in the mainstream flow. The size and position of the vortex zone are similar to the experimental results. In addition, an advanced analysis using Q and λ criteria, which serve to detect the vorticity and to deeper analyze the vortex zones, were implemented in the study. The Q and λ2 methods show that the vortex intensity is largest in the separation zone, where the large vorticity values result

from the change in flow direction. The vorticity values are larger in this zone than in the vortex region, where the vorticity remains rather weak. The Q criterion allows the shear motion and vortex zones to be distinguished. As a conclusion, just downstream of the baffle, there is, as expected, a vortex region but of weak intensity in comparison with the mainstream flow, where the strong vorticity value is generated by the flow direction change.

A hybrid computational and analytical model to predict the discharge of flat integrated PC drippers as a function of pressure and geometrical parameters was proposed by Narain and Winter (2019). A pressure resistance parameter was derived using an experimentally validated CFD model to describe the flow behavior in tortuous paths. An SST model was used for turbulence as it is suitable for cases in which flow separation and recirculating regions in the flow path are expected. The bending mechanics of the membrane were modeled analytically and refined by deriving a correction factor using finite element analysis. Simulations were run using ANSYS CFX 16.0. Three commercially available drippers were used for validation purposes. The combined hybrid computational-analytical model reduced the computational time of modeling emitters from hours to less than 30 min, dramatically lowering the time required to iterate and select optimal designs. Errors between the experimental and simulated discharges of the three commercially available drippers were lower than 12%. A more analytical approach for modeling PC drippers was reported previously by Shamshery *et al*. (2017).

The CFD numerical simulation of water-sediment two-phase flow in four different tooth channel structure emitters confirmed that different channel types have effects on the distribution of the flow velocity, turbulent kinetic energy, turbulent kinetic energy dissipation rate, and physical particle trajectory (YANG *et al*., 2020). Optimization of the channel structures increased the turbulent kinetic energy and the area of the main flow, enhancing the transport rate of physical particles and the clogging resistance of the emitters.

The hydraulic properties of an NPC flat dripper were estimated by CFD comparing turbulence models and wall functions (DEMİR *et al*., 2020). Simulations were performed using ANSYS Fluent 17.2. In this study, a realizable k-ε model with enhanced wall treatment, SST k-ω turbulence model with low-Re corrections and production limiter options, and Stress-Omega RSM with low-Re corrections and shear flow correction options were considered for the CFD analysis. The authors reported that the wall thickness of the drip irrigation pipe is an important parameter for emitter discharge. The emitter discharge was predicted to be very close to the experimental data with the proper choice of the turbulence model, wall function, and the well-configured mesh structure.

Computational fluid dynamics, an artificial neural network (ANN), and a multi-objective genetic algorithm (MOGA) were used to investigate the hydraulic performance of microporous ceramic emitters (MPCE) and conduct parameter optimization (ZHOU *et al*., 2020). A CFD software package was used to analyze the influence of the working parameters, structural parameters, and material properties on the flow characteristics of MPCE. Predictions of discharge were similar using the laminar model, the standard k-ε model, the RNG k- ε model, and the realizable k-ε model. Subsequently, an ANN and MOGA were used to optimize the fabrication cost, discharge, and flow index of the emitter.

Chemical scaling

In microirrigation systems, one of the factors that can cause complete or partial clogging of drippers is scaling caused by deposits of salts of low solubility, which are formed under certain physical-chemical conditions due to the presence of ions in irrigation water, such as Ca^{+2}, Mg^{+2}, Fe^{+2}, Mn^{+2}, HCO^{-}_{3}, CO^{-2}_{3}, PO^{-3}_{4} and SO^{-2}_{4}. These salts also commonly cause scaling on pipe walls, valves, and other irrigation equipment. Over time, the deposits can compromise the flow of water and equipment performance. Chemical precipitates are produced when certain physicochemical characteristics of the water (pH, total dissolved solids, temperature, and partial pressure of CO_2) are modified and, above all, by the evaporation of water in the emitters after irrigation, which increases the concentration of the dissolved salts that then precipitate when reaching the solubility limit. Scaling forms gradually and is therefore difficult to detect (HEATH *et al*., 2013; LAMM *et al*., 2006; NAKAYAMA *et al*., 1977; NAM *et al*., 2016; PALANISAMY; SUBRAMANIAN, 2016; PIZARRO CABELLO, 1996).

Calcium carbonate deposits are quite common in arid and semi-arid regions, whose irrigation waters are characterized by high hardness. The formation of calcium carbonate deposits begins with the change in the chemical equilibrium state of the solution, although the dynamic behavior of the crystal size and the hydraulic transport of these particles are also of great importance in scaling phenomena (MACIEL *et al*., 2019). The main stages related to calcium carbonate scaling are shown in Figure 4. Dissolved ions start nucleation with subsequent growth and agglomeration of the crystals until the incrustation itself is reached (COSMO *et al*., 2019).

The initial fouling stage (i.e., the induction period) is poorly understood due to the lack of experimental data (YANG, 2020). In recent last decades, an alternative that

has been used to better understand the induction period, as well as other phases present in scaling formation and thus fouling mitigation strategies, is the implementation of models using CFD, which considers that fouling is driven by a chemical reaction, precipitation, turbulent flow, and system operation time (BAYAT *et al*., 2012; CHENG *et al*., 2009; YANG, 2020).

The use of CFD to investigate the mechanisms of scaling and chemical precipitates is already well established in petroleum engineering and industrial sectors that use equipment for cooling or heating numerous fluids (e.g., heat exchangers and cooling towers) (BAYAT *et al*., 2012; BRAHIM *et al*., 2003a; CHENG *et al*., 2009; CHHANWAL *et al*., 2011; DAVOODY *et al*., 2018; HAN *et al*., 2019; KURIAKOSE; ANANDHARAMAKRISHNAN, 2010; LIM, 2002; MACIEL *et al*., 2019; PÄÄKKÖNEN *et al*., 2016; PITON *et al*., 2000; TENG *et al*., 2017; TROFA *et al*., 2019; WEI *et al*., 2001; YANG, 2020). However, no studies have been found in irrigation engineering that addresses the use of CFD in investigations of the scaling of chemical precipitates in emitters, pipes, or any irrigation equipment.

The CFD models available in commercial software seem to be useful for simulations with irrigation equipment. The results can provide relevant information such as the moment when there is scaling, the amount of mass deposited, and the moment when the deposit can interfere with the proper functioning of the system, causing a change in the flow parameters. In drip irrigation systems, for example, it would be interesting to know when scaling begins so that crystal growth inhibition procedures and maintenance procedures can be initiated, such as the application of acids. In addition, information on the amount of mass deposited for a certain scenario can be useful for calculating the quantity of products to be injected into the system for recovery purposes, thus avoiding the application of excessively large or insufficient amounts of chemicals for the reclamation of irrigation system components. This would lead to time and product savings, which would certainly minimize maintenance costs.

Several mathematical models of crystal inlay have been presented in the literature (BOTT, 1995; HASSON *et al*., 1968; LI *et al*., 1992; MACIEL *et al*., 2019; MWABA *et al*., 2006; PÄÄKKÖNEN *et al*., 2016; SAGHATOLESLAMI *et al*., 2010; SEGEV *et al*., 2012). Transport processes such as fluid flow, heat, and mass transfer can be described mathematically by the conservation equations that can be obtained from the balances of mass, amount of movement, and energy, but these partial differential equations can be solved analytically in simple cases only (PÄÄKKÖNEN *et al*., 2016). For more complex geometries, numerical methods such as the finite volume method, finite difference method, or finite element method can be used to solve the equations that govern the process. For the numerical resolution of these equations, CFD is usually used.

Some studies that use CFD to study scaling mechanisms are related to the heat exchangers commonly used in industries (BRAHIM; AUGUSTIN; BOHNET, 2003b, 2003a; DAVOODY *et al*., 2018; KHO; MÜLLER-STEINHAGEN, 1999; OLIEMANS, 1992; SAGHATOLESLAMI *et al*., 2010). Several studies that address CFD in fouling research use the method proposed by Saghatoleslami *et al*. (2010), who adopted user-defined functions through the commercially available ANSYS Fluent Software to study fouling processes.

Maciel *et al*. (2019) used CFD to predict $CaCO_3$ precipitation under oil well conditions with different geometric configurations. The authors confirmed the feasibility of applying CFD for the study of fluid dynamics in well equipment, obtaining consistent results from a physical and mathematical point of view, and suitable for field observations. The results of the simulations allowed the optimization of the well geometry in order to minimize the mass adhered to the internal surface of the studied control volume. The simulations also allowed the

Figure 4 - Main phenomena involved in calcium carbonate scaling (COSMO *et al*., 2019)

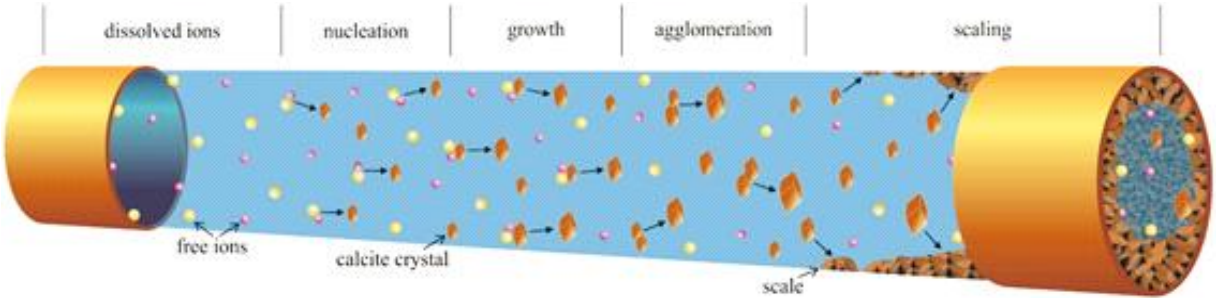

authors to verify the effect of the increase in flow rate on the scaling of $CaCO_3$. The authors also verified that the boundary conditions must be properly defined so that the results obtained in the simulations are approximated to reality.

The influence of hydrodynamics on the precipitation process of barium sulfate was studied using ANSYS Fluent 4.5 (LIM, 2002). The velocity and energy dissipation fields were solved by the Navier-Stokes equations together with the standard k-ε turbulence model. These equations and precipitation kinetics were implemented directly in the CFD using user-defined subroutines. The model was able to predict the effect of the flow rate on the average size of the crystal particles formed in the scaling process.

Brahim *et al*. (2003a, 2003b) integrated a model to study the deposition and removal of scaling in parallel plate-type heat exchangers using CFD. The authors used a mechanistic model for calcium sulfate. Applying a structured grid for the flow calculations between parallel flat plates, the authors considered both the velocity and the distribution of the heat flow (as a function of the total thickness of the layer) as time-dependent variables. To avoid the need for a moving contour approach, the authors considered a fictitious crystal growth model, which consists of varying the speed of entry of the heat flow as a function of the thickness of the encrusted layer, which is calculated through the relationship of the deposited mass (given by the deposition/suppression model) by its density.

Saghatoleslami (2010) simulated the fouling process by the crystallization of calcium sulfate in a heat exchanger by developing different models using ANSYS Fluent 6.1. The results obtained allowed the authors to evaluate the thickness and the fouling rate in the heat exchangers. In addition, the authors simulated the effect of pulsatile flow (i.e., Womersley flow) on the crystallization of calcium sulfate in the exchanger and also evaluated the effect of different amplitudes of oscillations (10–70) and different frequencies (1.59–12.73 Hz) on the fouling resistance. The simulation results allowed the authors to evaluate the effect of applying different treatments on the deposition and removal of the deposited mass. They observed the influence of the formation of vortices on the resistance to fouling. The variation in the amplitude and frequency of the pulsatile flow generated instability in the flow, forcing it to become unstable with the formation of vortices. The fouling resistance was reduced with increasing amplitude due to a higher flow rate. The increase in the pulsation amplitude led to a secondary shear layer, with the formation of pairing, fusion, and new vortices causing a concentration of high temperatures close to the tube wall owing to this effect. For the turbulent flow region, the increase in the frequency proportionally increased the resistance to fouling. The amplitude pulsation caused more turbulent fluctuation and therefore more shear stress on the heat transfer surface; thus, the rate of mass removal increased over time. It was also observed that the increase in the flow contributed to the increase in the removal of scaling.

Three-dimensional CFD-based simulations were performed under different operating conditions to evaluate fouling mechanisms and to directly predict deposition rates in heat exchangers (YANG, 2020). The effects of the variation in the temperature of the tube wall and the flow velocity on the rate of fouling formation, removal rate, and aging process were studied in a set of CFD simulations under various operational conditions. The results of the simulations allowed the evaluation of the effect of different flow conditions on the deposition rate and removal of asphaltenes in the flow pipe walls.

Bayat *et al*. (2012) used CFD to predict the fouling rate in an industrial crude oil preheater. The species transport model was applied to simulate the mixing and transport of chemical species. The possibility of the adhesion of reaction products to the wall was considered by applying a high viscosity to products in competition with the shear stress on the wall. The results indicated that the initial fouling layers developed after about nine days, and the thickness of the fouling layer increased over time. In the pipe inlet section, no severe fouling occurred, even during long periods of operation. However, the maximum amount of fouling was formed in the outlet section of the tube because of the longer residence time available for the reagents. As the fouling progressed, the available cross-sectional area was reduced. Finally, the simulation results indicated that the CFD model can predict the fouling rate in both the induction and fouling development periods.

Filters for irrigation

In microirrigation systems, solid particles are the major components of emitter clogging problems (ADIN; ALON, 1986; LAVANHOLI *et al*., 2018; LIU *et al*., 2016; NAKAYAMA; BUCKS, 1991; TAYLOR *et al*., 1995; YU *et al*., 2018) originating from the sediments and organic matter carried in suspension. Ideally, all suspended solid particles present in the water for irrigation should be removed by the filtering system. Nevertheless, practical and economical limitations only allow for the removal of larger particles and, consequently, sediments can be found in irrigation lines (LI *et al*., 2019; LI *et al*., 2015; PUIG-BARGUÉS; LAMM, 2013). The aggregation of small solid particles that escape filtration may occur under certain physicochemical and hydrodynamic conditions

(BOUNOUA *et al*., 2016; NIU *et al*., 2012; OLIVEIRA *et al*., 2020) as well as interactions with biological and chemical clogging agents (LAMM *et al*., 2006). Since the complete removal of suspended solid particles is cost prohibitive for microirrigation systems, one of the practical recommendations is to remove particles larger than $1/10^{th}$ of the smallest flow passage of the emitter (GOYAL *et al*., 2016). The selection, sizing, and maintenance of filter systems must be appropriate for the effective control of irrigation water, preventing clogging problems, maintaining application uniformity, and avoiding the increase in operational costs (TESTEZLAF, 2008).

Screen, disc, and media filters are usually required in microirrigation systems as well as complementary devices such as hydrocyclones. The screen filters (or strainer-type filters) have metallic or plastic housing that supports one or more filter elements. The filter element is a component consisting of a perforated plate, screen, mesh, or a combination of these that is intended to retain suspended solids larger than a specified aperture size. The screen can be made of steel, nylon, polypropylene, or non-woven materials. The characteristics of the screen, such as the diameter and shape of the wire, directly affect the fluid flow and performance of the filter (KANG *et al*., 2007). Screen filters are recommended for the elimination of fine sand, large inorganic elements, and small amounts of algae with organic matter (HAMAN; ZAZUETA, 2017). Automatic flushing filters have the initiation and termination of discrete flushing cycles activated automatically by means of differential pressure or at regular intervals of time or filtered volume (NAKAYAMA *et al*., 2007).

Disc filters have filter elements composed of discs with grooves of textured faces arranged one on top of the other to form a stack. The porous space between adjacent discs determines the size of the particles trapped by the filter element. The disc filter elements can be cleaned manually or automatically. During manual cleaning, the housing is removed, the shaft expands, and the compressed discs separate, which facilitates cleaning. In automatic cleaning systems, flushing is activated by differential pressure or at pre-defined time intervals, opening a flushing valve that allows water to flow through the discs, removing the particles trapped by the grooves (NAKAYAMA *et al*., 2007).

Media filters are cylindrical tanks or reservoirs capable of resisting static and dynamic pressures, in which a thick layer of sand is placed, through which the irrigation water is filtered (SALCEDO *et al*., 2011). Media filters are able to retain organic and inorganic materials in suspension (RAVINA *et al*., 1997). The retention of suspended solids in the porous medium occurs through three actions: sieving, sedimentation, and adhesion/ cohesion (PIZARRO CABELLO, 1996). Puig-Bargués *et al*. (2005) considered that filtration in sand filters is a deep filtration, in which the suspended material is retained by the pores of the filter medium, and particles that are smaller than the pores of the filter medium will be retained by physical mechanisms. Backwashing is a critical part of media filter operation and performance. The flow direction inside the filter is reversed to remove the particulate material adhered to the filter medium. The reverse flow velocity must be adequate to cause separation and suspension of the material. Expansion of the filter layer should be allowed, but the flow velocities should not be excessive in order to avoid the loss of material from the filter medium (NAKAYAMA *et al*., 2007).

Various tools and studies have emerged in recent years with the intention of improving designs, energy consumption, and knowing the behavior and efficiency of particle removal by filters (SOLÉ-TORRES *et al*., 2019). Computational fluid dynamics is a tool that allows hydrodynamic simulations of irrigation equipment and from which it is expected improvements in designs and an increase in performance will be obtained (PUJOL *et al*., 2020).

ANSYS Fluent was used to simulate the fluid flow across a screen filter (ZONG; ZHENG, 2012). The authors identified that the pressure distribution was not uniformly distributed, resulting in larger head losses and uneven clogging in the screen. The simulation results were not validated with experimental data.

Liming *et al*. (2018) simulated particle motion under different flow rates and diameters in screen filters. The small particles initially managed to pass through the screen, but were retained by the accumulation of larger particles, aggravating the clogging of the pores of the medium that had formed on the surface of the screen. Reducing the inlet velocity increased the uniformity of the particle distribution, enhanced the auxiliary effect of the filter cake, and prolonged the effective time and the operational life span of the filter. The non-uniform distribution of sediments led to a local blockage in the filter element.

Yang *et al*. (2018) examined the fluid flow characteristics of a two-stage filtration system composed of a sand filter and a screen filter for irrigation systems. Pro/Engineer was used for 3D modeling, and the CFD numerical simulation adopted the RNG k-ε model combined with a porous media model.

Arbat *et al*. (2011) used CFD to compute the head losses in different parts of a sand filter. Simulations were performed using ANSYS Fluent. The results indicated that not only was the filtration media responsible for the total

head losses but also the auxiliary elements, such as the filter nozzles and the inlet/outlet pipes.

In order to determine the effect of the backwashing on a media filter, Kim *et al*. (2011) evaluated three backwash models from the use of four parameters: turbidity of the backwash waste, mass of suspended solids in backwash waste, head loss development, and initial turbidity breakthrough.

Bové *et al*. (2015) used CFD to analyze the elements and regions that produce the most pressure drop in a sand filter. In addition, a new underdrain was designed to reduce the pressure loss and reduce the pressure drop of the entire filter by 35%. Improved underdrain elements could increase energy efficiency and reduce the sand media pressure drop. Fluid flow simulations were carried out using ANSYS Fluent, and the standard k-ε turbulence model was used.

Three commercial sand filter models were evaluated experimentally to investigate the effects of the internal auxiliary elements (the diffuser plate and the underdrains) and their interaction with the sand particle size and media bed depth on the head loss as a function of the water flow velocity under clean water conditions (MESQUITA *et al*., 2012). The different internal auxiliary elements significantly affected the head loss. The head loss values were significantly affected by the sand particle size, bed depth, filtration velocity, and the interactions among these variables. Mesquita *et al.* (2017) used CFD to identify the profile and homogeneity of the distribution of flow lines and characterize the trend of flow during the filtration and backwash processes for different underdrain types (nozzles) used in pressurized sand filters. The results showed that the commercial models (cylindrical and conical) provided uneven distribution flow lines, and flux stagnation points were identified. An optimized underdrain was proposed, and it presented better distribution homogeneity of the flow lines. Simulations were run using ANSYS CFX using the standard k-ε model. Furthermore, Mesquita *et al.* (2019) designed and evaluated the hydrodynamic performance of a sand filter equipped with a novel diffuser plate using numerical simulations. In addition, the three commercial sand filters reported by Mesquita *et al.* (2012) were analyzed. For the three commercial diffuser plates and flow velocities evaluated, a tendency to generate a vortex and a tangential flow on the sand bed surface was observed, which caused sand movement inside the equipment with the formation of accumulation points and the creation of preferred paths for water and suspended solids. The new diffuser plate reduced the internal flow kinetic energy and vortex formation, improving the flow uniformity in the sand bed surface with reduced bed deformation.

Bové *et al.* (2017) designed a new underdrain capable of reducing pressure loss by 50% compared with commercial filters (taken as references), especially under backwash conditions. ANSYS Fluent was used for the CFD numerical simulation. Wand-type underdrains were studied using CFD (PUJOL *et al*., 2020). The spatial distribution of the wand-type underdrains was identified as a key parameter in the hydraulic performance of sand filters.

Computational fluid dynamics was used to simulate the flow characteristics of a hydrocyclone filter (YANG *et al*., 2018). The objective was to analyze the effects of different inlet flow rates and inlet concentrations on the solid-liquid separation performance. The geometries of the equipment were modified along the tests. The obtained results were the turbulence inside the separation device as well as the fluid velocity, in addition to the solid-liquid separation efficiency.

Rainer and Ho (2002) simulated a 3D flow across a filter with horizontal rotating discs to investigate the influence of the shaped scrapers between the discs on flow parameters such as dissipation, turbulence, and overflow velocities. Simulations were performed using Gambit for meshing generation and ANSYS Fluent for fluid flow simulation. Simulations comparing the RNG k-ε and the RSM indicated that the first model presented lower computing requirements and satisfactory accuracy for this application.

Castilho and Anspach (2003) designed a rotation disk filter that was able to separate mammalian cells, avoiding membrane fouling and cell damage. The authors analyzed different geometries and variables of the rotating disk. Variables such as the rotor radius, rotor angle, membrane rotor distance, and angular velocities were investigated. The CFD simulations were performed using ANSYS Fluent and the RSM turbulence model and standard wall function. The CFD results provided correlations describing the average shear stress on the membrane surface and the maximum shear stress in the whole module as a function of the variables studied.

The fluid flow parameters of a rotation disk structure in a rotating-disk dynamic filter were examined by Hwang and Wu (2015) for microalgae separation. Three dimensional fluid flow fields were simulated for various rotating disks, disk rotation speeds, and feed flow rates using ANSYS Fluent and the RNG k-ε model. The authors found that the disk structure and rotation speed were the most crucial factors affecting the filtration performance.

Sprinklers

Atomization (the process of forming droplets from a liquid core jet) is found in many industrial processes, such

as engine injection systems, ink jet printers, and sprinkler irrigation. This widely used irrigation technique is based on turbulent jets of water that have very high Reynolds and Weber numbers and developed over several tens of meters, aiming at transporting water over large distances. Over these distances, the initial liquid jet core breaks down, giving rise to a very large number of liquid pieces of various sizes, ranging from a few tens of micrometers to several millimeters. Ultimately, droplets of various sizes are created in the far field. Statistically, their description is provided by a histogram or droplet number density.

Sprinkler irrigation efficiency is strongly related to the homogeneity of the water spray on the irrigated surface and losses due to wind drift and evaporation (up to 30%). Furthermore, poor irrigation management may lead to soil degradation by erosion and compaction. All these processes depend on both the dynamics and fragmentation of the spray and its dispersion. Improving the performance of sprinkler irrigation systems and reducing water losses requires better control of atomization and transport mechanisms and, initially, better characterization of the sprays produced. Such concerns are crucial in the context of sprinkler irrigation with treated or reclaimed wastewater. Sprinkler irrigation systems were not developed for using poor quality waters, and irrigation strategies still do not offer clear cut solutions to the users of such waters (MOLLE *et al*., 2012). The application efficiency requires limiting drift because the smallest droplets are poorly characterized (MOLLE *et al*., 2016; TOMAS *et al*., 2019) and generated by the sprinklers, often in interaction with wind.

For jets with large diameters, such as those used for sprinkler irrigation, primary atomization is slightly affected by aerodynamic effects when the liquid to gas density ratio is higher than 500. The atomization in this case is governed by the turbulence of the liquid; the liquid surface is disturbed by the scales of turbulence having sufficient energy to overcome surface tension forces. It is the smallest of these scales that form ligaments on the surface of the liquid at the nozzle outlet. Then, as the distance of the jet from the nozzle increases and small turbulent scales are dissipated, the liquid column is deformed by increasingly large turbulent scales. The deformation of the column gives rise to three-dimensional structures (SALLAM; FAETH, 2003). The aerodynamic forces acting on them augment until column fragmentation occurs via secondary atomization mechanisms (HOYT; TAYLOR, 1977; SALLAM *et al*., 2002). The spray produced is composed of droplets resulting from primary and secondary atomization mechanisms, and larger elements stemming from the fragmentation of the liquid column. These fragments progressively break up as they move in the air.

Recent measurements and simulations (FELIS *et al.*, 2020; STEVENIN *et al*., 2016) have shown that the turbulent droplet motion in the spray is strongly anisotropic, with values of the anisotropy coefficient (ratio of transverse to longitudinal velocity variances) lower than 0.2. This anisotropy is unexpected because other studies on sprays (generally concerned with engine applications) show a relatively low anisotropy. This strong anisotropy is responsible for the poor radial dispersion of the spray, but it may also have other consequences on the spray properties (in terms of droplet sizes, for instance).

In some situations (for $x/d < 1000$), the "equivalent single-phase fluid" approach (STEVENIN *et al*., 2016) provides a general description of the water-air jet under some assumptions. Its main advantage is the limited numerical resources and good agreement between the near and intermediate fields. In this description, the droplet sizes are provided through the Sauter mean diameter and the transport is considered based on the average droplet size. For the far field, the latter assumption is unrealistic. The mixture model is a simpler alternative to the previous model because the fluids are considered as a continuum.

Other irrigation equipment

Finally, other applications of CFD simulations were found for direct-acting pressure-regulating valves and in Venturi injectors.

A numerical simulation of the flow in a direct-acting pressure-regulating valve for irrigation purposes was performed by Zhang and Li (2017). Numerical simulations considering the movement of the regulating plunger were run using ANSYS Fluent. The effects of the geometrical and spring parameters and their interactions on the preset pressure and the slope of the performance line of the unregulated segment were revealed.

The hydraulic characteristics of four Venturi injector prototypes have been studied using CFD ANSYS Fluent (MANZANO *et al*., 2014). According to the authors, CFD techniques appear to be a suitable tool for the analysis of Venturi injector operation, but validation with experimental data is recommended.

CONCLUSIONS

1. Computational fluid dynamics uses in irrigation engineering must be encouraged, particularly for innovation purposes resulting from cooperation between academia and irrigation companies;
2. The applications briefly described indicated that CFD modeling can be an accurate, quick, and less expensive

method for investigating flow parameters in irrigation pipes, fittings, emitters, and accessories. The CFD simulations can be useful for designing new products as well as for improving and optimizing existing products. For development purposes, CFD may reduce the number of prototypes manufactured for preliminary evaluations, decreasing investment, time, and labor needs. Although experimental data are always essential for validation purposes, CFD might reduce laboratory trials and their corresponding investments.

ACKNOWLEDGEMENTS

The authors are grateful to the São Paulo State Scientific Foundation (FAPESP-Brazil, Project 2018/20099-5) and to Unicamp-FAEPEX (Projects N. 2022/19 and 3081/19) for financial support, and to the USP-COFECUB program of academic cooperation between French and Brazilian researchers (Project No. 2015-3). We would like to thank Editage (www.editage.com) for English language editing.

REFERENCES

ADIN, B. A.; ALON, G. Mechanisms and process parameters of filter screens. **Journal of Irrigation and Drainage Engineering**, v. 112, n. 4, p. 293-304, 1986.

AL-MUHAMMAD, J.; TOMAS, S.; AIT-MOUHEB, N.; AMIELH, M.; ANSELMET, F. Experimental and numerical characterization of the vortex zones along a labyrinth milli-channel used in drip irrigation. **International Journal of Heat and Fluid Flow**, v. 80, p. 1-11, 2019.

ARBAT, G.; PUJOL, T.; MONTORO, L.; *et al*. Using Computational Fluid Dynamics to Predict Head Losses in the Auxiliary Elements of a Microirrigation Sand Filter. **Transactions of the ASABE**, v. 54, n. 4, p. 1367-1376, 2011.

BARTZANAS, T.; KACIRA, M.; ZHU, H.; *et al*. Computational fluid dynamics applications to improve crop production systems. **Computers and Electronics in Agriculture**, v. 93, p. 151-167, 2013.

BAYAT, M.; AMINIAN, J.; BAZMI, M.; SHAHHOSSEINI, S.; SHARIFI, K. CFD modeling of fouling in crude oil pre-heaters. Energy Conversion and Management. **Anais...** . v. 64, p.344-350, 2012

BOMBARDELLI, W. W. Á.; CAMARGO, A. P. DE; FRIZZONE, J. A.; LAVANHOLI, R.; ROCHA, H. S. DA. Local head loss caused in connections used in micro-irrigation systems. **Revista Brasileira de Engenharia Agrícola e Ambiental**, v. 23, n. 7, p. 492-498, 2019.

BOTT, T. R. **Fouling of Heat Exchangers**. New York: Elsevier, 1995.

BOUNOUA, S.; TOMAS, S.; LABILLE, J.; *et al*. Understanding physical clogging in drip irrigation: in situ, in-lab and numerical approaches. **Irrigation Science**, v. 34, n. 4, p. 327-342, 2016.

BOVÉ, J.; ARBAT, G.; PUJOL, T.; *et al*. Reducing energy requirements for sand filtration in microirrigation: Improving the underdrain and packing. **Biosystems Engineering**, v. 140, p. 67-78, 2015.

BOVÉ, J.; PUIG-BARGUÉS, J.; ARBAT, G.; *et al*. Development of a new underdrain for improving the efficiency of microirrigation sand media filters. **Agricultural Water Management**, v. 179, p. 296-305, 2017.

BRAHIM, F.; AUGUSTIN, W.; BOHNET, M. Numerical simulation of the fouling process. **International Journal of Thermal Sciences**, v. 42, p. 323-334, 2003a.

BRAHIM, F.; AUGUSTIN, W.; BOHNET, M. **Numerical Simulation of the Fouling on Structured Heat Transfer Surfaces (Fouling)**. 2003b.

CASTILHO, L. R.; ANSPACH, F. B. CFD-aided design of a dynamic filter for mammalian cell separation. **Biotechnology and Bioengineering**, v. 83, n. 5, p. 514-524, 2003.

CELIK, H. K.; KARAYEL, D.; LUPEANU, M. E.; RENNIE, A. E. W.; AKINCI, I. Determination of head losses in drip irrigation laterals with cylindrical in-line type emitters through CFD analysis. **Bulgarian Journal of Agricultural Science**, v. 21, n. 3, p. 703-710, 2015.

CHENG, J.; YANG, C.; MAO, Z. S.; ZHAO, C. CFD modeling of nucleation, growth, aggregation, and breakage in continuous precipitation of barium sulfate in a stirred tank. **Industrial and Engineering Chemistry Research**, v. 48, n. 15, p. 6992-7003, 2009.

CHHANWAL, N.; INDRANI, D.; RAGHAVARAO, K. S. M. S.; ANANDHARAMAKRISHNAN, C. Computational fluid dynamics modeling of bread baking process. **Food Research International**, v. 44, n. 4, p. 978-983, 2011.

COSMO, R. DE P.; RESSEL PEREIRA, F. DE A.; RIBEIRO, D. DA C.; BARROS, W. Q.; MARTINS, A. L. Estimating CO2 degassing effect on CaCO3 precipitation under oil well conditions. **Journal of Petroleum Science and Engineering**, v. 181, p. 1-8, 2019.

DAVOODY, M.; LANE, G.; GRAHAM, L. J. W.; *et al*. Scale formation on the wall of a mechanically stirred vessel-experimental assessment and interpretation using computational fluid dynamics. **AIChE Journal**, v. 64, n. 11, p. 3912–3922, 2018.

DEMIR, V.; YURDEM, H.; DEGIRMENCIOGLU, A. Development of Prediction Models for Friction Losses in Drip Irrigation Laterals equipped with Integrated In-line and On-line Emitters using Dimensional Analysis. **Biosystems Engineering**, v. 96, n. 4, p. 617-631, 2007.

DEMIR, V.; YÜRDEM, H.; YAZGI, A.; GÜNHAN, T. Measurement and Prediction of Total Friction Losses in Drip Irrigation Laterals with Cylindrical Integrated in-line Drip

Emitters using CFD Analysis Method. **Tarım Bilimleri Dergisi**, v. 25, n. 3, p. 354-366, 2019.

DEMİR, V.; YÜRDEM, H.; YAZGI, A.; GÜNHAN, T. Determination of the Hydraulic Properties of a Flat Type Drip Emitter using Computational Fluid Dynamics. **Journal of Agricultural Sciences**, v. 26, n. 2, p. 226-235, 2020.

FALCUCCI, G.; KRASTEV, V. K.; BISCARINI, C. Multi-component Lattice Boltzmann simulation of the hydrodynamics in drip emitters m m er ci us e m m er al on. **Journal of agricultural Engineering**, v. 48, n. 649, p. 175-180, 2017.

FELIS, F.; TOMAS, S.; VALLET, A.; AMIELH, M.; ANSELMET, F. Experimental analysis of the flow characteristics of a pressure-atomised spray. **International Journal of Heat and Fluid Flow**, v. 85, n. September 2019, p. 108624, 2020.

FENG, J.; LI, Y.; WANG, W.; XUE, S. Effect of optimization forms of flow path on emitter hydraulic and anti-clogging performance in drip irrigation system. **Irrigation Science**, v. 36, n. 1, p. 37-47, 2018.

FRIZZONE, J. A.; FREITAS, P. S. L.; REZENDE, R.; FARIA, M. A. **Microirrigação: gotejamento e microaspersão**. 1 ed. Maringá: Eduem, 2012.

GOROKHOVSKI, M.; HERRMANN, M. Modeling primary atomization processes. **Annu. Rev. Fluid. Mech.**, v. 40, p. 343-366, 2008.

GOYAL, M. R.; CHAVAN, V. K.; TRIPATHI, V. K. **Principles and management of clogging in micro irrigation**. Boca Raton: Apple Academic Press, 2016.

HAMAN, D. Z.; ZAZUETA, F. S. **Screen Filters in Trickle Irrigation Systems**. Florida , US, 2017.

HAN, Z.; XU, Z.; YU, X. CFD modeling for prediction of particulate fouling of heat transfer surface in turbulent flow. **International Journal of Heat and Mass Transfer**, v. 144, p. 118-428, 2019.

HASSON, D.; AVRIEL, M.; RESNICK, W.; ROZENMAN, T.; WINDREICH, S. Calcium carbonate scale deposition on heat transfer surfaces. **Desalination**, v. 5, n. 1, p. 107-119, 1968.

HEATH, D.; ŠIROK, B.; HOCEVAR, M.; PECNIK, B. The use of the cavitation effect in the mitigation of CaCO3 Deposits. **Strojniski Vestnik/Journal of Mechanical Engineering**, v. 59, n. 4, p. 203-215, 2013.

HOYT, J. W.; TAYLOR, J. J. Waves on water jets. **Journal of Fluid Mechanics**, v. 83, n. 1, p. 119-127, 1977.

HWANG, K.-J.; WU, S.-E. Disk structure on the performance of a rotating-disk dynamic filter: A case study on microalgae microfiltration. **Chemical Engineering Research and Design**, v. 94, n. 2011, p. 44-51, 2015.

KANG, J. W.; KIM, J. A.; KIM, E. Y.; *et al*. CFD Analysis of Liquid Stream Going Through the Wire-Screen Mesh. 5th International Conference on Heat Transfer, Fluid Mechanics and Thermodynamics. **Anais...** . v. HEFAT2007, p.1–5, 2007. Sun City, South Africa.

KHO, T.; MÜLLER-STEINHAGEN, H. An experimental and numerical investigation of heat transfer fouling and fluid flow in flat plate heat exchangers. **Chemical Engineering Research and Design**, v. 77, n. 2, p. 124-130, 1999.

KIM, S. H.; LIM, H. K.; JEONG, W. C.; PARK, N. S. Optimum backwash method for granular media filtration of seawater. **Desalination and Water Treatment**, v. 32, n. 1-3, p. 431-436, 2011.

KURIAKOSE, R.; ANANDHARAMAKRISHNAN, C. Computational fluid dynamics (CFD) applications in spray drying of food products. **Trends in Food Science and Technology**, v. 21, n. 8, p. 383-398, 2010.

KURIAN, M.; REZA, A. **Governing the Nexus: Water, soil and waste resources considering global change**. 1 ed. London: Springer, 2015.

LAMM, F. R.; AYARS, J. E.; NAKAYAMA, F. S. **Microirrigation for crop production: design, operation and management**. Amsterdam: Elsevier, 2006.

LAVANHOLI, R.; CAMARGO, A. P.; BOMBARDELLI, W. W. Á.; *et al*. Prediction of pressure-discharge curves of trapezoidal labyrinth channels from nonlinear regression and artificial neural networks. **Journal of Irrigation and Drainage Engineering**, v. 146, n. 8, p. 1-10, 2020.

LAVANHOLI, R.; OLIVEIRA, F. C.; CAMARGO, A. P.; *et al*. Methodology to Evaluate Dripper Sensitivity to Clogging due to Solid Particles: An Assessment. **The Scientific World Journal**, p. 1-9, 2018.

LEE, I. B.; BITOG, J. P. P.; HONG, S. W.; *et al*. The past, present and future of CFD for agro-environmental applications. **Computers and Electronics in Agriculture**, v. 93, p. 168-183, 2013.

LI, G. Y.; J. D. WANG; M. ALAM; Y. F. ZHAO. Influence of geometrical parameters of labyrinth flow path of drip emitters on hydraulic and anti-clogging performance. **Transactions of the ASABE**, v. 49, n. 3, p. 637-643, 2006.

LI, Q.; DUNN, E. T.; GRANDMAISON, E. W.; GOOSEN, M. F. A. Applications and Properties of Chitosan. **Journal of Bioactive and Compatible Polymers**, v. 7, n. 4, p. 370-397, 1992.

LI, Q.; SONG, P.; ZHOU, B.; *et al*. Mechanism of intermittent fluctuated water pressure on emitter clogging substances formation in drip irrigation system utilizing high sediment water. **Agricultural Water Management**, v. 215, p. 16-24, 2019.

LI, Y. K.; YANG, P. L.; XU, T. W.; *et al*. Hydraulic property and flow characteristics of three labyrinth flow paths of drip irrigation emitters under micro-pressure. **Transactions of the ASABE**, v. 52, n. 4, p. 1129-1138, 2009.

LI, Y.; LIU, H.; YANG, P.; WU, D. Analysis of tracing ability of different sized particles in drip irrigation emitters with computational fluid dynamics. **Irrigation and Drainage**, v. 62, n. 3, p. 340-351, 2013.

LI, Y.; SONG, P.; PEI, Y.; FENG, J. Effects of lateral flushing on emitter clogging and biofilm components in drip irrigation

systems with reclaimed water. **Irrigation Science**, v. 33, n. 3, p. 235-245, 2015.

LI, Y.; YANG, P.; REN, S.; XU, T. Hydraulic characterization of tortuous flow in path drip irrigation emitter. **Journal of Hydrodynamics, Ser. B**, v. 18, n. 4, p. 449-457, 2006.

LI, Y.; YANG, P.; XU, T.; *et al*. CFD and digital particle tracking to assess flow characteristics in the labyrinth flow path of a drip irrigation emitter. **Irrigation Science**, v. 26, n. 5, p. 427-438, 2008.

LIM, C. N. CFD simulation of precipitation process. **Recent Advances in Computational Science and Engineering**, p.188-191, 2002.

LIMING, Y.; ZHOU, X.; JURUI, Y.; *et al*. Numerical Simulation of Water and Sediment Movement in Screen Filter Based on Coupled CFD-DEM. **Transactions of the chinese Society of Agricultural Engineering**, v. 49, n. 3, p. 303-308, 2018.

LIU, H.; SUN, H.; LI, Y.; *et al*. Visualizing Particle Movement In Flat Drip Irrigation Emitters With Digital Particle Image Velocimetry. **Irrigation and Drainage**, v. 65, n. 4, p. 390-403, 2016.

MACIEL, R. S.; ASSIS, F. DE; PEREIRA, R.; FEJOLI, R. F. Enhancing Scale Prediction in Pre-Salt Wells Using Numerical Simulation. **SPE Annual Technical Conference and Exhibition**, Alberta - Canada, 2019.

MANZANO, J.; AZEVEDO, B. M. DE; BOMFIM, G. V. DO; *et al*. Diseño y predicción del funcionamiento de inyectores Venturi en riego localizado. **Revista Brasileira de Engenharia Agrícola e Ambiental**, v. 18, n. 12, p. 1209-1217, 2014.

MARTÍ, P.; PROVENZANO, G.; ROYUELA, Á.; PALAU-SALVADOR, G. Integrated Emitter Local Loss Prediction Using Artificial Neural Networks. **Journal of Irrigation and Drainage Engineering**, v. 136, n. 1, p. 11-22, 2010.

MÉNARD, T.; TANGUY, S.; BERLEMONT, A. Coupling level set/VOF/ghost fluid methods: Validation and application to 3D simulation of the primary break-up of a liquid jet. **International Journal of Multiphase Flow**, v. 33, n. 5, p. 510-524, 2007.

MESQUITA, M.; DE DEUS, F. P.; TESTEZLAF, R.; DA ROSA, L. M.; DIOTTO, A. V. Design and hydrodynamic performance testing of a new pressure sand filter diffuser plate using numerical simulation. **Biosystems Engineering**, v. 183, p. 58-69, 2019.

MESQUITA, M.; TESTEZLAF, R.; DE DEUS, F. P.; DA ROSA, L. M. Characterization of flow lines generated by pressurized sand filter underdrains. **Chemical Engineering Transactions**, v. 58, n. 2010, p. 715-720, 2017.

MESQUITA, M.; TESTEZLAF, R.; RAMIREZ, J. C. S. The effect of media bed characteristics and internal auxiliary elements on sand filter head loss. **Agricultural Water Management**, v. 115, p. 178-185, 2012.

MOLLE, B.; BRELLE, F.; BESSY, J.; GATEL, D. Which water quality for which uses? Overcoming over-zealous use of the precautionary principle to reclaim wastewater for appropriate irrigation uses. **Irrigation and Drainage**, v. 61, n. SUPPL.1, p. 87-94, 2012.

MOLLE, B.; TOMAS, S.; HUET, L.; *et al*. Experimental Approach to Assessing Aerosol Dispersion of Treated Wastewater Distributed via Sprinkler Irrigation. **Journal of Irrigation and Drainage Engineering**, v. 142, n. 9, p. 1-8, 2016.

MWABA, M. G.; GOLRIZ, M. R.; GU, J. A semi-empirical correlation for crystallization fouling on heat exchange surfaces. **Applied Thermal Engineering**, v. 26, n. 4, p. 440-447, 2006.

NAKAYAMA, F. S.; BOMAN, B. J.; PITTS, D. J. **Microirrigation for Crop Production**. Amsterdam: Elsevier, 2007.

NAKAYAMA, F. S.; BUCKS, D. A. Water quality in drip/trickle irrigation: A review. **Irrigation Science**, v. 12, n. 4, p. 187-192, 1991.

NAKAYAMA, F. S.; BUCKS, D. A.; FRENCH, O. F. Reclaiming partially clogged trickle emitters. **Transactions of the ASABE**, v. 20, n. 2, p. 278-280, 1977.

NAM, H.; BAI, C.; SHIM, J.; CHO, Y. I. A study on the reduction of CaCO3fouling in hot-water storage tank by short pulse plasma application (rev 1 yc). **Applied Thermal Engineering**, v. 102, p. 108-114, 2016.

NARAIN, J.; WINTER, A. G. A Hybrid Computational and Analytical Model of Inline Drip Emitters. **Journal of mechanical design**, v. 141, p. 1-13, 2019.

NIJDAM, J. J.; GUO, B.; FLETCHER, D. F.; LANGRISH, T. A. G. Lagrangian and Eulerian models for simulating turbulent dispersion and coalescence of droplets within a spray. **Applied Mathematical Modelling**, v. 30, n. 11, p. 1196-1211, 2006.

NISHIMURA, T.; OHORI, Y.; KAWAMURA, Y. Flow characteristics in a channel with symmetric wavy wall for steady flow. **Journal of Chemical Engineering of Japan**, v. 17, n. 5, p. 466-471, 1984.

NIU, W.; LIU, L.; CHEN, X. Influence of fine particle size and concentration on the clogging of labyrinth emitters. **Irrigation Science**, v. 31, n. 4, p. 545-555, 2012.

NORTON, T. CFD in the Agri-Food Industry: A maturing engineering design tool. **Computers and Electronics in Agriculture**, v. 93, p. 149-150, 2013.

OLIEMANS, R. V. A. **Computational fluid dynamics for the petrochemical process industry**. 1992.

OLIVEIRA, F. C.; LAVANHOLI, R.; CAMARGO, A. P.; *et al*. Clogging of drippers caused by suspensions of kaolinite and montmorillonite clays. **Irrigation Science**, v. 38, n. 1, p. 65–75, 2020.

PÄÄKKÖNEN, T. M.; OJANIEMI, U.; PÄTTIKANGAS, T.; *et al*. CFD modelling of CaCO3 crystallization fouling on heat transfer surfaces. **International Journal of Heat and Mass Transfer**, v. 97, p. 618-630, 2016.

PALANISAMY, K.; SUBRAMANIAN, V. K. CaCO3 scale deposition on copper metal surface; effect of morphology, size

and area of contact under the influence of EDTA. **Powder Technology**, v. 294, p. 221-225, 2016.

PALAU-SALVADOR, G.; SANCHIS, L. H.; GONZÁLEZ-ALTOZANO, P.; ARVIZA-VALVERDE, J. Real Local Losses Estimation for On-Line Emitters Using Empirical and Numerical Procedures. **Journal of Irrigation and Drainage Engineering**, v. 132, n. 6, p. 522-530, 2006.

PALAU SALVADOR, G.; ARVIZA VALVERDE, J.; BRALTS, V. F. Hydraulic Flow Behaviour through an In-line Emitter Labyrinth using CFD Techniques. ASAE/CSAE Annual International Meeting. **Anais...** . p.8, 2004. Ottawa, Canada: American Society of Agricultural and Biological Engineers.

PATANKAR, N. A.; JOSEPH, D. D. Lagrangian numerical simulation of particulate flows. **International Journal of Multiphase Flow**, v. 27, n. 10, p. 1685-1706, 2001.

PERBONI, A.; FRIZZONE, J. A.; CAMARGO, A. P. DE; PINTO, M. F. Modelling head loss along emitting pipes using dimensional analysis. **Engenharia Agrícola**, v. 35, n. 3, p. 442-457, 2015.

PITON, D.; FOX, R. O.; MARCANT, B. Simulation of fine particle formation by precipitation using computational fluid dynamics. **Canadian Journal of Chemical Engineering**, v. 78, n. 5, p. 983-993, 2000.

PIZARRO CABELLO, F. **Riegos localizados de alta frecuencia**. 3º ed. Bilbao: Ediciones Mundi-Prensa, 1996.

POPE, S. B. **Turbulent flows**. Cambridge: Cambridge University Press, 2000.

PROVENZANO, G.; ALAGNA, V.; AUTOVINO, D.; JUAREZ, J. M.; RALLO, G. Analysis of geometrical relationships and friction losses in small-diameter lay-flat polyethylene pipes. **Journal of Irrigation and Drainage Engineering**, v. 142, n. 2, p. 1-9, 2016.

PROVENZANO, G.; DIO, P. DI; SALVADOR, G. P. New Computational Fluid Dynamic Procedure to Estimate Friction and Local Losses in Coextruded Drip Laterals. **Journal of Irrigation and Drainage Engineering**, v. 133, n. 6, p. 520-527, 2007.

PUIG-BARGUÉS, J.; BARRAGÁN, J.; RAMÍREZ DE CARTAGENA, F. Filtration of effluents for microirrigation systems. **Transactions of the ASAE**, v. 48, n. 3, p. 969-978, 2005.

PUIG-BARGUÉS, J.; LAMM, F. R. Effect of Flushing Velocity and Flushing Duration on Sediment Transport in Microirrigation Driplines. **Transactions of the ASABE**, p. 1821-1828, 2013.

PUJOL, T.; PUIG-BARGUÉS, J.; ARBAT, G.; *et al*. Effect of wand-type underdrains on the hydraulic performance of pressurised sand media filters. **Biosystems Engineering**, v. 192, p. 176-187, 2020.

QINGSONG, W.; GANG, L.; JIE, L.; *et al*. Evaluations of emitter clogging in drip irrigation by two-phase flow simulations and laboratory experiments. **Computers and Electronics in Agriculture**, v. 63, n. 2, p. 294-303, 2008.

RAINER, M.; HO, W. 3D-flow simulation and optimization of a cross flow filtration with rotating discs. **Separation and Purification Technology**, v. 26, p. 121-131, 2002.

RAVINA, I.; PAZ, E.; SOFER, Z.; *et al*. Control of clogging in drip irrigation with stored treated municipal sewage effluent. **Agricultural Water Management**, v. 33, n. 2-3, p. 127-137, 1997.

SAGHATOLESLAMI, N.; SALOOKI, M. K.; ARMIN, M. A. Prediction of thickness and fouling rate in pulsating flow heat exchangers, using FLUENT simulator. **Korean Journal of Chemical Engineering**, v. 27, n. 1, p. 96-103, 2010.

SALCEDO, J. C.; TESTEZLAF, R.; MESQUITA, M. Processo de retrolavagem em filtros de areia usados na irrigação localizada. **Engenharia Agrícola**, v. 31, n. 6, p. 1226-1237, 2011.

SALLAM, K. A.; DAI, Z.; FAETH, G. M. Liquid breakup at the surface of turbulent round liquid jets in still gases. **International Journal of Multiphase Flow**, v. 28, n. 3, p. 427-449, 2002.

SALLAM, K. A.; FAETH, G. M. Surface Properties During Primary Breakup of Turbulent Liquid Jets in Still Air. **AIAA Journal**, v. 41, n. 8, p. 1514-1524, 2003.

SEGEV, R.; HASSON, D.; SEMIAT, R. Rigorous modeling of the kinetics of calcium carbonate deposit formation. **AIChE Journal**, v. 58, n. 4, p. 1222-1229, 2012.

SHAMSHERY, P.; WANG, R.-Q.; TRAN, D. V.; WINTER V, A. G. Modeling the future of irrigation: A parametric description of pressure compensating drip irrigation emitter performance. (A. Aliseda, Org.). **PLOS ONE**, v. 12, n. 4, p. 1-24, 2017.

SOBENKO, L. R.; BOMBARDELLI, W. W. Á.; CAMARGO, A. P.; FRIZZONE, J. A.; DUARTE, S. N. Minor Losses through Start Connectors in Microirrigation Laterals: Dimensional Analysis and Artificial Neural Networks Approaches. **Journal of Irrigation and Drainage Engineering**, v. 146, n. 5, p. 1-13, 2020.

SOLÉ-TORRES, C.; PUIG-BARGUÉS, J.; DURAN-ROS, M.; *et al*. Effect of underdrain design, media height and filtration velocity on the performance of microirrigation sand filters using reclaimed effluents. **Biosystems Engineering**, v. 187, p. 292-304, 2019.

STEVENIN, C.; VALLET, A.; TOMAS, S.; AMIELH, M.; ANSELMET, F. Eulerian atomization modeling of a pressure-atomized spray for sprinkler irrigation. **International Journal of Heat and Fluid Flow**, v. 57, p. 142-149, 2016.

TAYLOR, H.; BASTOS, R.; PEARSON, H.; MARA, D. Drip irrigation with waste stabilisation pond effluents: Solving the problem of emitter fouling. **Water Science and Technology**, v. 31, n. 12, p. 417-424, 1995.

TENG, K. H.; KAZI, S. N.; AMIRI, A.; *et al*. Calcium carbonate fouling on double-pipe heat exchanger with different heat exchanging surfaces. **Powder Technology**, v. 315, p. 216-226, 2017.

TESTEZLAF, R. Filtros de areia aplicados à irrigação localizada: teoria e prática. **Engenharia Agricola**, v. 28, n. 3, p. 604-613, 2008.

TOMAS, S.; MOLLE, B.; CHEVARIN, C.; SERRA-WITTLING, C. Transport Modeling in Sprinkler Irrigation. **Journal of Irrigation and Drainage Engineering**, v. 145, n. 8, p. 1-9, 2019.

TROFA, M.; D'AVINO, G.; SICIGNANO, L.; *et al*. CFD-DEM simulations of particulate fouling in microchannels. **Chemical Engineering Journal**, v. 358, p. 91-100, 2019.

VILAÇA, F. N.; DE CAMARGO, A. P.; FRIZZONE, J. A.; MATEOS, L.; KOECH, R. Minor losses in start connectors of microirrigation laterals. **Irrigation Science**, v. 35, n. 3, p. 227-240, 2017.

WALLER, P.; YITAYEW, M. **Irrigation and Drainage Engineering**. New York: Springer, 2016.

WANG, Y.; ZHU, D.; ZHANG, L.; ZHU, S. Simulation of Local Head Loss in Trickle Lateral Lines Equipped with In-line Emitters Based on Dimensional Analysis. **Irrigation and Drainage**, v. 67, n. 4, p. 572-581, 2018.

WEI, H.; ZHOU, W.; GARSIDE, J. Computational fluid dynamics modeling of the precipitation process in a semibatch crystallizer. Industrial and Engineering Chemistry Research. **Anais...** . v. 40, p. 5255-5261, 2001.

WEI, Q.; SHI, Y.; DONG, W.; LU, G.; HUANG, S. Study on hydraulic performance of drip emitters by computational fluid dynamics. **Agricultural Water Management**, v. 84, n. 1, p. 130-136, 2006.

WEI, Z.; DU, J.; YUAN, W.; ZHAO, G. Fluid-structure interaction analysis on pressure-compensating emitters. **Applied Engineering in Agriculture**, v. 30, n. 5, p. 783-788, 2014.

WU, D.; LI, Y.; LIU, H.; *et al*. Simulation of the flow characteristics of a drip irrigation emitter with large eddy methods. **Mathematical and Computer Modelling**, v. 58, n. 3-4, p. 497-506, 2013.

YANG, B.; WANG, J.; ZHANG, Y.; *et al*. Anti-clogging performance optimization for dentiform labyrinth emitters. **Irrigation Science**, v. 38, p. 275-285, 2020.

YANG, J. Computational fluid dynamics studies on the induction period of crude oil fouling in a heat exchanger tube. **International Journal of Heat and Mass Transfer**, v. 159, p. 1-15, 2020.

YANG, P.; ZHOU, Y.; REN, S.; MA, Z. Structural optimization and performance test of Sand - Screen combination filter. **Transactions of the chinese Society of Agricultural Engineering**, v. 49, n. 10, p. 307-316, 2018.

YANG, Z.; SHIH, T. H.; SHIHT, T. H. New time scale based κ- ε model for near-wall turbulence. **AIAA Journal**, v. 31, n. 7, p. 1191-1198, 1993.

YU, L.; LI, N.; LIU, X.; *et al*. Influence of Dentation Angle of Labyrinth Channel of Drip Emitters on Hydraulic and Anti-Clogging Performance. **Irrigation and Drainage**, v. 68, n. 2, p. 256-267, 2019.

YU, L.; LI, N.; LONG, J.; LIU, X.; YANG, Q. The mechanism of emitter clogging analyzed by CFD–DEM simulation and PTV experiment. **Advances in Mechanical Engineering**, v. 10, n. 1, p. 1-10, 2018.

YU, L.; LI, N.; YANG, Q.; LIU, X. Influence of Flushing Pressure before Irrigation on the Anti-Clogging Performance of Labyrinth Channel Emitters. **Irrigation and Drainage**, v. 67, n. 2, p. 191-198, 2018.

ZHANG, C.; LI, G. Optimization of a direct-acting pressure regulator for irrigation systems based on CFD simulation and response surface methodology. **Irrigation Science**, v. 35, n. 5, p. 383-395, 2017.

ZHANG, J.; ZHAO, W.; TANG, Y.; LU, B. Anti-clogging performance evaluation and parameterized design of emitters with labyrinth channels. **Computers and Electronics in Agriculture**, v. 74, n. 1, p. 59-65, 2010.

ZHANG, J.; ZHAO, W.; TANG, Y.; LU, B. Structural optimization of labyrinth-channel emitters based on hydraulic and anti-clogging performances. **Irrigation Science**, v. 29, n. 5, p. 351-357, 2011.

ZHANG, J.; ZHAO, W.; WEI, Z.; TANG, Y.; LU, B. Numerical and experimental study on hydraulic performance of emitters with arc labyrinth channels. **Computers and Electronics in Agriculture**, v. 56, n. 2, p. 120-129, 2007.

ZHANGZHONG, L.; YANG, P.; LI, Y.; REN, S. Effects of Flow Path Geometrical Parameters on Flow Characteristics and Hydraulic Performance of Drip Irrigation Emitters. **Irrigation and Drainage**, v. 65, n. 4, p. 426-438, 2016.

ZHANGZHONG, L.; YANG, P.; REN, S.; LIU, Y.; LI, Y. Flow Characteristics and Pressure-Compensating Mechanism of Non-Pressure-Compensating Drip Irrigation Emitters. **Irrigation and Drainage**, v. 64, n. 5, p. 637-646, 2015.

ZHOU, W.; ZHANG, L.; WU, P.; *et al*. Hydraulic performance and parameter optimisation of a microporous ceramic emitter using computational fluid dynamics, artificial neural network and multi-objective genetic algorithm. **Biosystems Engineering**, v. 189, n. 22, p. 11-23, 2020.

ZITTERELL, D. B.; FRIZZONE, J. A.; RETTORE NETO, O. Dimensional analysis approach to estimate local head losses in microirrigation connectors. **Irrigation Science**, v.32, p.169-179, 2013.

ZONG, Q. L.; ZHENG, T. G. Numerical Simulation on Flow Field of Screen Filter for Drip Irrigation in Field. **Applied Mechanics and Materials**, v. 212–213, p. 1197-1200, 2012.